Astronomy & Astrophysics manuscript no. paper 2nd February 2008
(DOI: will be inserted by hand later)

Long-term evolution of compact binaries with irradiation feedback

Andreas Büning and Hans Ritter

Max-Planck-Institut für Astrophysik, Karl-Schwarzschild-Str. 1, D-85740 Garching, Germany

received/accepted

Abstract We resume the discussion about irradiation-driven mass transfer cycles in semi-detached compact binary systems. The analytical model that describes the onset of these cycles, which occur on a thermal timescale of the donor star, is reexamined. We take into account a contribution of the thermal relaxation which is not related to the irradiation of the donor star and which was neglected in previous studies. Cataclysmic variables (CVs) containing extended giant donors are more stable than previously thought. CVs close to the upper edge of the period gap can undergo cycles for low angular momentum loss rates, as they have been suggested by recent magnetic braking prescriptions, while they are stable for high braking rates.
A model for the irradiation geometry that takes into account surface elements near the terminator of the donor star indicates that possibly also low-mass X-ray binaries (LMXBs) can undergo mass transfer cycles. Regarding the braking rate, which is necessary to drive cycles, basically the same restrictions apply for short period LMXBs as they do for short period CVs. We confirm that LMXBs containing giants can undergo cyles. In terms of an irradiation efficiency parameter α CVs are susceptible to the irradiation instability for $\alpha \gtrsim 0.1$ while LMXBs are susceptible for $\alpha \lesssim 0.1$.
The predictions of the analytical model are checked by the first long-term evolutionary computations of systems undergoing mass transfer cycles with full 1D stellar models. For unevolved main sequence (MS) and giant donors the analytic model provides reasonable values for the boundaries of the stable and unstable regions while CVs containing highly evolved MS donors are more stable at high braking rates than expected.
Taking into account irradiation the minimum period of CVs is increased by up to 1-2 minutes, depending on α.

Key words. binaries: close – novae, cataclysmic variables – stars: evolution – stars: mass-loss – X-rays: binaries

1. Introduction

Observations of close binary systems have shown that a star which is illuminated by its companion can exhibit a hotter, illuminated, and a cooler, unilluminated side (see, e.g., Eddington 1926; Ritter et al. 2000, and references therein). This is the well-known reflection effect (for a review see Vaz 1985). If the illuminated star has a convective envelope, then irradiation inhibits the energy transport through the illuminated outer layers (Vaz & Nordlund 1985). In the case of a semi-detached compact binary system the reflection effect can be caused by accretion luminosity that is released nearby the compact star. In this case the energy transport, i.e., the intrinsic flux through the illuminated outer layers of the donor star is coupled to the mass transfer rate. This leads to a feedback, the consequences of which are the subject of this paper.

The influence of irradiation onto mass transfer was first discussed by Podsiadlowski (1991) for the simplified case of symmetrical irradiation of the donor. Later, Hameury et al. (1993) tried to simulate asymmetrical irradiation by time-periodic symmetric irradiation and concluded that a more realistic model is required.

In a series of papers Ritter et al. (1995, 1996); King et al. (1995, 1996) developed a feedback model for asymmetrical irradiation that predicts under which conditions the secular mass transfer rate becomes unstable and the system undergoes mass transfer cycles which occur on a thermal timescale of the convective envelope of the donor star.

We reexamine the above-mentioned irradiation feedback model and take into account a contribution of the thermal relaxation which is not related to the irradiation of the donor star. It turns out that this term, which was neglected in previous studies of the above-mentioned analytical model, can become important, especially for giant donors.

Unfortunately, there have been basically no numerical computations to test the validity of this model and especially the boundaries of the stable and unstable regions. Only few computations have been carried out by using bipolytrope stellar models and in most cases also by using simplified models for the treatment of irradiation (Ritter et al. 1995; McCormick & Frank 1998; Ritter et al. 2000). There has been only one short-term evolution using full 1D stellar models and a realistic treatment of irradiation which was published by

Send offprint requests to: Hans Ritter,
e-mail: hsr@mpa-garching.mpg.de

Hameury & Ritter (1997). It has served more as a "proof of concept" for their model of the reduction of the intrinsic flux by illumination than as a numerical confirmation of the irradiation feedback model.

The main purpose of this paper is to confirm the predictions of the irradiation feedback model by numerical long-term evolutionary computations that are based on full 1D stellar models for the donor star, a realistic model for the irradiation geometry, and tabulated results of Hameury & Ritter (1997) for the reduction of the intrinsic flux by illumination.

In Sect. 2 we mention the input physics that is necessary for the feedback model and for the numerical computations. This includes the mass loss rate prescription, the reflection effect, the irradiation geometry, and the thermal relaxation of the donor star. Afterwards, in Sect. 3 we develop two ordinary differential equations which describe the system adequately for our purpose, and in Sect. 4 we derive the conditions which describe the onset of instability by means of linear stability analysis.

We give a short overview in Sect. 5 about input physics, which we use in our code, and subsequently, we present our numerical results for CVs and LMXBs containing evolved and unevolved donor stars in Sect. 6.

2. Input physics

We consider a semi-detached compact binary system. The compact primary star, a white dwarf, a neutron star, or a black hole, is denoted by subscript 1, the secondary star, a main sequence star with a convective envelope or a giant, by subscript 2. Both stars move on circular orbits with an orbital distance A. We assume that the secondary corotates with the orbital motion. This is justified by the short timescales of orbital circulatization and synchronization for such systems (e.g., Zahn 1977). The mass ratio of both stars is defined as

$$q = \frac{M_2}{M_1}. \tag{1}$$

The secondary almost fills its critical Roche lobe and therefore loses mass through the inner Lagrangian point L_1 to its compact companion.

2.1. The mass transfer rate

Since the donor star does not have a sharp rim, the mass loss rate must be a continuous function of the difference

$$\Delta R = R_2 - R_{\mathrm{R},2} \tag{2}$$

between the radius R_2 and the Roche radius $R_{\mathrm{R},2}$ of the star. For computing the mass loss rate we use

$$\dot{M}_2 = -\dot{M}_0 \exp\left(\frac{\Delta R}{H_{\mathrm{P}}}\right), \tag{3}$$

where $\dot{M}_0 > 0$ is a weakly varying function of the system parameters M_1, M_2, A, and the photospheric values of the donor, and H_{P} denotes the photospheric pressure scale height (for details see Ritter 1988). Strictly speaking, Eq. (3) is applicable only to a donor star which slightly underfills its Roche lobe. This is the case for most of the systems we are interested in. In any case, the conclusions of this paper are independent of the exact form of the mass transfer prescription as long as the characteristic scale length H, on which $\dot{M}_2$ increases by a factor of e, fulfills

$$H := \left(\frac{1}{\dot{M}_2}\frac{\mathrm{d}\dot{M}_2}{\mathrm{d}\Delta R}\right)^{-1} \ll R_2. \tag{4}$$

We note that in (3) the characteristic scale length is $H = H_{\mathrm{P}}$ and that $\frac{H_{\mathrm{P}}}{R_2}$ is of order $\sim 10^{-4}$ for low-mass MS stars and up to $\sim 10^{-2}$ for giants.

2.2. The accretion geometry and the irradiating flux

We assume that the matter streaming through the L_1-point is collected in an accretion disk surrounding the primary and that a fraction $0 \le \eta \le 1$ of the transferred matter is finally accreted, i.e.:

$$\dot{M}_1 = -\eta\dot{M}_2. \tag{5}$$

The fraction $1 - \eta$ is lost from the system and carries away angular momentum, which is parametrized in terms of

$$\nu = \frac{\mathrm{d}\ln J}{\mathrm{d}\ln M}, \tag{6}$$

where J is the orbital angular momentum and $M = M_1 + M_2$ the total mass of the system. This mode of orbital angular momentum loss is usually referred to as consequential angular momentum loss (CAML, see, e.g., King & Kolb 1995). If the matter is lost with the specific orbital angular momentum of the primary, then $\nu = q$.

The accretion process releases gravitational energy and produces accretion luminosity, mostly on or nearby the compact star so that the source of the accretion luminosity can be treated as a point source. Hence, the irradiating flux at a distance d is given by

$$F_{\mathrm{irr}} = \frac{\alpha_{\mathrm{accr}}}{4\pi d^2}\frac{\Gamma M_1}{R_1}\dot{M}_1. \tag{7}$$

Γ is the gravitational constant, and α_{accr} takes into account that the gravitational energy is not necessarily completely released as accretion luminosity and that the accretion luminosity is not necessarily radiated isotropically with respect to the primary.

On the long term the system can lose additional matter and angular momentum, e.g., by nova explosions so that the long-term average value $\overline{\eta}$ can be less than η, even $\overline{\eta} < 0$ is possible (e.g., Hameury et al. 1989; Prialnik & Kovetz 1995). In this case $\overline{\eta}$ determines the (long-term) mass and angular momentum balance while η determines the momentary accretion rate and therefore the accretion luminosity. As has been shown by Schenker et al. (1998), describing the long-term evolution by an average $\overline{\eta}$ is reasonable.

2.3. The reflection effect and the intrinsic flux

A star that is illuminated by its companion shows a reflection effect (for a review see Vaz 1985). Accordingly, the star has

an illuminated, brighter and hotter side with an irradiation-dependend effective temperature $T_{\rm irr}$ and an unilluminated, darker and cooler side with an effective temperature T_0. The intrinsic flux $F_{\rm int}$ through a surface element is defined as the net flux, i.e., the difference between the incoming flux $F_{\rm irr}$ and the outgoing flux $\sigma T_{\rm irr}^4$, where σ denotes the Stephan-Boltzmann constant. It is convenient to write the irradiating flux in units of the intrinsic flux $F_0 = \sigma T_0^4$ on the unilluminated side:

$$f_{\rm irr} = \frac{F_{\rm irr}}{F_0}. \tag{8}$$

Typically, the reflection effect is discussed in terms of the bolometric reflection albedo

$$w_{\rm bol} = \frac{\sigma T_{\rm irr}^4 - \sigma T_0^4}{F_{\rm irr}} \tag{9}$$

but for the purpose of this paper it is more convenient to use the intrinsic flux in units of F_0:

$$f_{\rm int} = \frac{F_{\rm int}}{F_0} = \frac{\sigma T_{\rm irr}^4 - F_{\rm irr}}{F_0} = \frac{T_{\rm irr}^4}{T_0^4} - f_{\rm irr}. \tag{10}$$

For stars in radiative equilibrium the irradiating flux $f_{\rm irr}$ is reprocessed and completely reemitted. They show $w_{\rm bol} = 1$ and $f_{\rm int} = 1$ all over the surface. Stars with convective envelopes are by definition not in radiative equilibrium and for them $w_{\rm bol}$ and $f_{\rm int}$ can be less than unity.

Convection in the interior of stars is efficient, i.e., adiabatic. It was first stated by Ruciński (1969) that the entropy, which is constant in the adiabatic convection zone, must determine the intrinsic flux through the outer layers. This means that, as was first recognized by Vaz & Nordlund (1985), the temperature gradient must be flatter on the illuminated, hotter side than on the unilluminated, cooler side: Since the temperature gradient in the adiabatic convection zone is essentially tied to the adiabatic temperature gradient, the temperature gradient in the subphotospheric, superadiabatic layers must be flatter on the illuminated side. Therefore, energy transport through the illuminated outer layers is inhibited. In fact, the superadiabatic zone acts like a valve for the energy flow. This can be unterstood in terms of a simple one-zone model (Ritter et al. 1995, 2000).

Ritter et al. (2000, App. A) have pointed out that lateral energy transport within the superadiadiabatic convection zone is negligible since the radial temperature gradient in the superadiabatic layers is much larger than the lateral temperature gradient. Hence, irradiation can be treated as a local effect and for every surface element separately. While this is most likely a good approximation for weak irradiation, i.e., typical CVs, it is possible that for sufficiently strong irradiation, i.e., typical LMXBs, non-local effects like circulations, which transport heat from the illuminated to the unilluminated side, become non-negligible. We will discuss this topic in more detail in Sec. 6.4.

By solving the equations of stellar structure for an unirradiated and an irradiated surface element simultaneously for a fixed entropy at the bottom of the adiabatic zone it is possible to compute $f_{\rm int}\,(f_{\rm irr})$ numerically. This has been done by Hameury & Ritter (1997)[1] for grey atmospheres and perpendicular irradiation for a large grid of effective temperature T_0 and surface gravity $g = \frac{\Gamma M_2}{R_2^2}$. The results are available in tabular form and we use them for our numerical calculations.

The assumption of a grey atmosphere and an irradiated Planck spectrum is not necessarily very accurate, especially for CVs and LMXBs. Various properties like a different penetration depth of optical light, UV and X-rays are neglected. A smaller penetration depth means that the external radiation field is mainly absorbed and reprocessed in the optically thin[2] layers of the atmosphere. This reduces the effect of the irradiation on the photospheric boundary conditions and therefore the intrinsic flux is less inhibited. This "efficiency" of the irradiation for a non-grey atmosphere compared to a grey atmosphere will be taken into account formally by a free parameter $\alpha_{\rm irr}$. If the external radiation field has the same spectrum as the irradiated star, then $\alpha_{\rm irr}$ is unity by definition. In the case of LMXBs hard X-rays, which can penetrate into the subphotospheric layers, can be the dominant component of the irradiating spectrum. But since even in the case of a grey atmosphere (i.e., $\alpha_{\rm irr} = 1$) about $\exp\left(-\frac{2}{3}\right) \approx \frac{1}{2}$ of the irradiating flux penetrates directly down to the photosphere at an optical depth of $\tau = \frac{2}{3}$ (see e.g., Tout et al. 1989, Eq. 29) and since even hard X-rays, except for the most energetic photons, do not penetrate sufficiently deep into the outer layers (Hameury 1996), we do not expect that $\alpha_{\rm irr}$ can become significantly greater than unity in typical LMXBs. Therefore, in general $\alpha_{\rm irr} \lesssim 1$.

Models of non-grey atmospheres irradiated by Planck spectra (Nordlund & Vaz 1990; Brett & Smith 1993) and real stellar spectra (Barman & Hauschildt 2001, 2002; Barman 2002) have been computed. However, those computations are much too time-consuming for generating tables that would be applicable for our purpose, i.e., similar to those by Hameury & Ritter (1997). Nevertheless, it is possible to compare models of irradiated non-grey atmospheres with models of irradiated grey atmospheres to get an estimate for the irradiation efficiency $\alpha_{\rm irr}$.

Since $f_{\rm int}$ depends on the penetration depth, irradiation is more efficient for a smaller opacity and thus for a smaller metallicity. Fig. 1 shows $f_{\rm int}$ as a function of metallicity for a specific binary system. Since the source radiates mainly in the optical, the results for grey atmospheres (crosses) do not differ much from those for non-grey atmospheres of the irradiated star, for an irradiated Planck spectrum (triangles) as well as for a real stellar spectrum (diamonds). The data shown are taken from Nordlund & Vaz (1990, table 1) and are compared with results from Hameury & Ritter (1997) (asterisk).

The reduction of $f_{\rm int}$ by irradiation also depends on the model of convection, especially the mixing length l as shown in Fig. 2. The data are taken from Nordlund & Vaz (1990, table 2) and Hameury & Ritter (1997).

[1] Those authors denote $f_{\rm irr}$ by x, $f_{\rm int}$ by $G(x)$ and $\frac{{\rm d}f_{\rm int}}{{\rm d}f_{\rm irr}}$ by $-g(x)$.

[2] "Optically thin" means optically thin for the outgoing radiation field. The same atmospheric layers can be optically thick for the incoming radiation field.

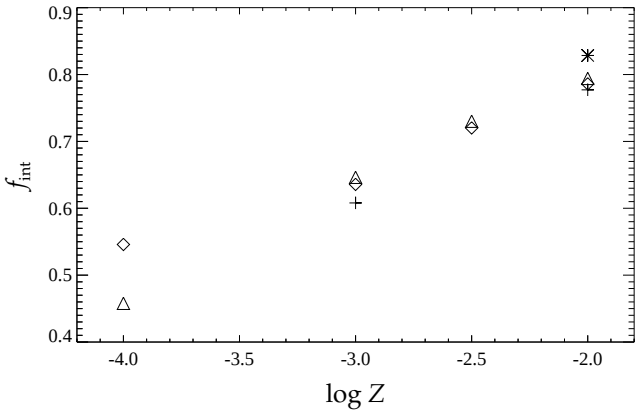

Figure 1. The intrinsic flux $f_{\rm int}$ as function of metallicity Z for a star with $T_0 = 4\,500$ K and an effective gravity $\log g = 4.5$ that is irradiated by $f_{\rm irr} \approx 1.006$ with an angle of incidence $\beta = 47.9°$, i.e., effectively by $f_{\rm irr} \approx 0.674$. The star is irradiated by its companion with $T_1 = 6\,000$ K and a relative radius of $\frac{R_1}{A} = \frac{1}{\sqrt{\pi}}$. The data shown are taken from Hameury & Ritter (1997) (asterisk) and Nordlund & Vaz (1990, table 1): grey atmospheres (crosses), and non-grey atmospheres irradiated by a Planck spectrum (triangles) and a real stellar spectrum (diamonds).

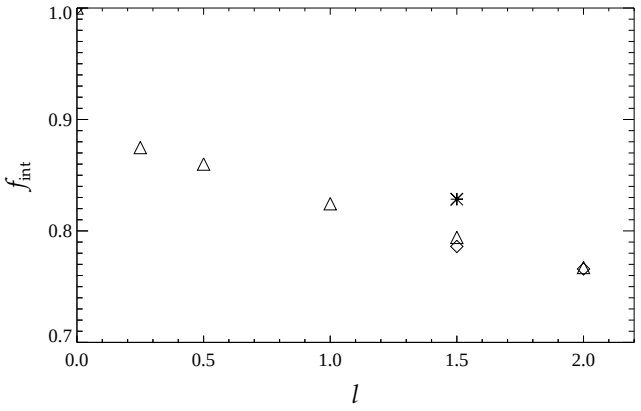

Figure 2. The intrinsic flux $f_{\rm int}$ as function of the mixing length l in units of the pressure scale height $H_{\rm P}$. Otherwise see Fig. 1.

For a plane-parallel atmosphere the external radiation field as a function of optical depth τ and angle of incidence β is given by

$$f_{\rm irr}(\tau,\beta) = f_{\rm irr}(0,0)\,\cos\beta\,\exp\left(-\frac{\tau}{\cos\beta}\right), \tag{11}$$

where $f_{\rm irr}(0,0)$ is the irradiating flux at $\tau = 0$ (Brett & Smith 1993). Fig. 3 shows $f_{\rm int}$ as function of β. The data from Nordlund & Vaz (1990, table 3) have been computed for $f_{\rm irr} \approx 1.006$ and different values of β while the data from Hameury & Ritter (1997) are formally valid only for perpendicular irradiation. The corresponding data points (asterisks) were computed for perpendicular irradiation with an "effective" flux $f_{\rm irr}\cos\beta$. Since Fig. 3 does not show any significant difference for large angles of incidence ($\cos\beta \to 0$), our treatment of an effective flux $f_{\rm irr}\cos\beta$ seems to be reasonable.

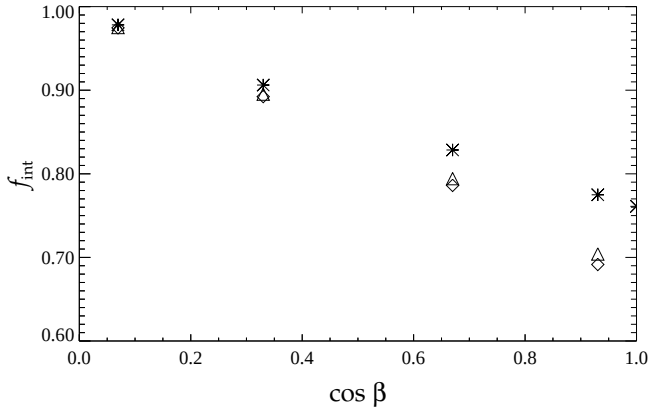

Figure 3. The intrinsic flux $f_{\rm int}$ as function of the angle of incidence β. Otherwise see Fig. 1.

Since $f_{\rm irr}$ can fluctuate on short timescales and the relation between $f_{\rm int}$ and $f_{\rm irr}$ is non-linear, the effect of irradiation does not only depend on the average $f_{\rm irr}$, but also on the amplitude and period of those fluctuations. This is taken into account formally by another free parameter $\alpha_{\rm d} \le 1$ which addresses the duty cycle of the irradiation. For constant irradiation $\alpha_{\rm d}$ is unity. For time-varying irradiation the efficiency depends on the (time-averaged) blocked part of the intrinsic flux $f_{\rm blocked} := 1 - f_{\rm int}$ which determines the heating of the convective envelope. Since $f_{\rm int}$ is a convex function for typical stellar envelopes as shown by Fig. 4, i.e.,

$$f_{\rm int}\left(a_1 f_{\rm irr,1} + a_2 f_{\rm irr,2}\right) \le a_1 f_{\rm int}\left(f_{\rm irr,1}\right) + a_2 f_{\rm int}\left(f_{\rm irr,2}\right) \tag{12}$$

for any $a_1, a_2 > 0$, $a_1 + a_2 = 1$, which is equivalent to $f''_{\rm int} \ge 0$, the efficiency and therefore $\alpha_{\rm d}$ decreases for non-constant irradiation. Splitting a mean $f_{\rm irr}$ into two phases of $f_{\rm irr,1}$ and $f_{\rm irr,2}$ increases the resulting mean $f_{\rm int}$ and thus decreases $f_{\rm blocked}$. If the illumination oscillates between an "On" state with high fluxes ($f_{\rm int} \approx 0$) and an "Off" state with $f_{\rm irr} \approx 0$, then we get

$$\alpha_{\rm d} \approx \frac{\tau_{\rm on}}{\tau_{\rm on} + \tau_{\rm off}}, \tag{13}$$

where $\tau_{\rm on}$ and $\tau_{\rm off}$ denote the average duration of the "On" and the "Off" state, respectively. We conclude that, e.g., nova-like variables have $\alpha_{\rm d} \approx 1$ while dwarf novae can have $\alpha_{\rm d} \ll 1$ in case of long quiescent phases between outbursts.

In the following we will use the symbol $f_{\rm irr}$, respectively $F_{\rm irr}$ for the effective irradiating flux

$$f_{\rm irr} = \frac{F_{\rm irr}}{F_0} = -\frac{\alpha\eta}{4\pi d^2 \sigma T_0^4}\frac{\Gamma M_1}{R_1}\dot{M}_2 \tag{14}$$

instead of (7), where the total efficiency α is defined as

$$\alpha = \alpha_{\rm d}\alpha_{\rm irr}\alpha_{\rm accr} \tag{15}$$

and $\dot{M}_1$ is replaced by (5).

Model No.	1	2	3	4	5	6
X_c	0.71	0.71	0.71	0.05	0.36	0
$M_2/M_\odot$	0.3	0.5	0.8	0.45	0.60	0.8
$R_2/R_\odot$	0.284	0.436	0.694	0.695	0.755	25.81
$\log T_0$/K	3.552	3.590	3.705	3.648	3.738	3.582
$\log L/L_\odot$	-1.93	-1.41	-0.54	-0.77	-0.34	2.10
M_{ce}/M_2	1.0	0.23	0.04	0.17	0.035	0.63
$10^4 H_P/R_2$	0.84	1.00	1.50	2.2	2.2	41.1
ζ_s	-0.31	-0.08	1.12	0.60	2.4	0.14
ζ_e	0.70	1.04	0.90	0.76	1.45	-0.2

Table 1. Values of several stellar models. No. 1-3 are unevolved MS stars, 4 is a remnant of thermal timescale mass transfer of an evolved MS star with an initial mass of 1.5 $M_\odot$, an initial central hydrogen abundance of 0.06, an initially 0.6 $M_\odot$ white dwarf primary, $\overline{\eta} = 0.25$, and subsequent mass loss driven by strong braking according to Verbunt & Zwaan (1981) using $f_{VZ} = 1$. No. 5 is similar but with an initial mass of 3 $M_\odot$, an initial central hydrogen abundance of 0.41, an initially 1.4 $M_\odot$ neutron star primary, and $\overline{\eta}$ is determined by an Eddington accretion rate of $2 \cdot 10^{-8}\, M_\odot$/yr, otherwise $\overline{\eta} = 1$. No. 6 is a giant.

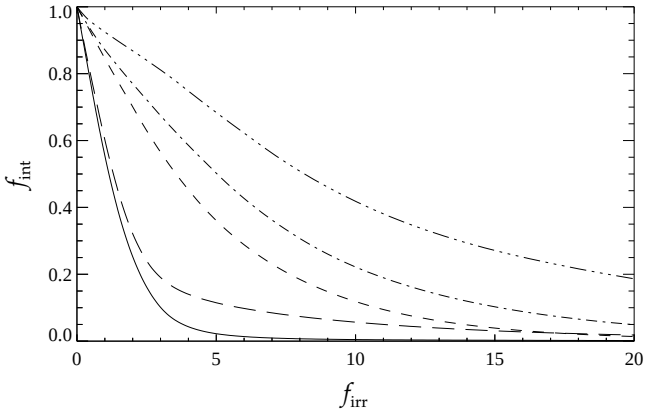

Figure 4. f_{int} for models no. 1-4 and 6 of table 1 (solid, long-dashed, short-dashed, dash-dotted and dot-dash-dotted line, respectively).

2.4. The irradiation geometry

2.4.1. The effectively blocked surface fraction

Using the definition of f_{int} in (10) the net luminosity of the star is given by

$$L_{int} = \int_0^{2\pi} \int_0^{\pi} f_{int}\,(f_{irr})\ \sigma T_0^4 R_2^2\ \sin\vartheta\,\mathrm{d}\vartheta\,\mathrm{d}\varphi, \tag{16}$$

but it is more convenient to write L_{int} as a function of R_2 and T_0 on the unirradiated side and an effectively blocked fraction of the surface s:

$$L_{int} = 4\pi(1-s)R_2^2\sigma T_0^4 \tag{17}$$

with

$$s = \frac{1}{4\pi}\int_0^{2\pi}\int_0^{\pi} [1 - f_{int}\,(f_{irr})]\ \sin\vartheta\,\mathrm{d}\vartheta\,\mathrm{d}\varphi. \tag{18}$$

(17) is a modified Stephan-Boltzmann equation for an asymmetrically irradiated star. The star is described as if a fraction s of its surface were completely blocked by the irradiation and a fraction $1 - s$ were unirradiated. Eq. (17) allows us to describe an asymmetrically irradiated star by a 1 D stellar model where the equations of stellar structure are solved "on the unilluminated side".

Due to the axial symmetry of the external radiation field (18) can be simplified:

$$s = \frac{1}{2}\int_0^{\vartheta_{max}} [1 - f_{int}\,(f_{irr})]\ \sin\vartheta\,\mathrm{d}\vartheta. \tag{19}$$

The maximum fraction of the surface that can be blocked by irradiation is determined by the system geometry. As can be seen from Fig. 5, only surface elements with $0 \le \vartheta < \vartheta_{max}$ are illuminated while surface elements with $\vartheta_{max} \le \vartheta \le \pi$ can not see the source. ϑ_{max} is defined by

$$\cos\vartheta_{max} = \frac{R_2}{A}. \tag{20}$$

Since $f_{int} = 1$ on unirradiated surface elements and $f_{int} \ge 0$ on irradiated surface elements, (19) yields the maximum value of s:

$$s \le \frac{1}{2}\int_0^{\vartheta_{max}} \sin\vartheta\,\mathrm{d}\vartheta = \frac{1}{2}\,(1 - \cos\vartheta_{max}) =: s_{max}. \tag{21}$$

Obviously, we have $s_{max} \le \frac{1}{2}$, and for typical system parameters it is of order of 0.3 – 0.4.

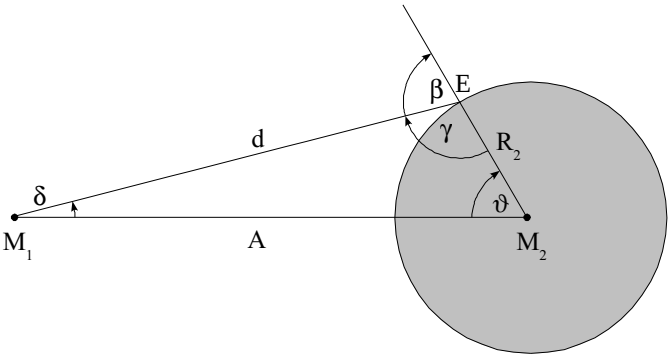

Figure 5. Irradiation geometry. A surface element E is irradiated by the source with an angle of incidence β to the surface normal.

2.4.2. The constant flux model

The simplest conceivable irradiation model is the constant flux model (Ritter et al. 1995, 2000) which assumes that f_{irr} has the constant average value

$$f_{irr} = \frac{1}{2}\langle f_{irr}\rangle := -\frac{\alpha\eta}{8\pi A^2\sigma T_0^4}\frac{\Gamma M_1}{R_1}\dot{M}_2 \tag{22}$$

over the irradiated surface where $\langle f_{irr}\rangle$ denotes the irradiating flux at a distance A according to (14). Then (19) yields:

$$s = s_{max}\,[1 - f_{int}\,(\langle f_{irr}\rangle)]\,. \tag{23}$$

2.4.3. The point source model

A more realistic model is the point source model (King et al. 1996; Ritter et al. 2000) where the irradiation source is treated as a point source as shown in Fig. 5. In this case the effective flux for a surface element E is given by

$$f_{\rm irr} = -\frac{\alpha\eta}{4\pi A^2\sigma T_0^4}\frac{\Gamma M_1}{R_1}\dot{M}_2\cos\beta = \langle f_{\rm irr}\rangle\cos\beta, \tag{24}$$

where $\cos\beta$ can be expressed by

$$\cos\beta = \frac{\cos\vartheta - \cos\vartheta_{\rm max}}{(1-2\cos\vartheta\cos\vartheta_{\rm max}+\cos^2\vartheta_{\rm max})^{\frac{3}{2}}} =: h(\vartheta). \tag{25}$$

2.5. Thermal relaxation

At turn-on of mass transfer and thus of irradiation a certain effective fraction s of the surface of the donor star is immediately blocked by irradiation. As a consequence the star is out of thermal equilibrium because the (unchanged) nuclear energy production $L_{\rm nuc} = L_0$ is higher than the (reduced) intrinsic luminosity $L_{\rm int} = (1-s)L_0$. The reaction of a star to spontaneous blocking of its intrinsic luminosity has been discussed by Spruit (1982) in connection with star spots: On short timescales the changes of the photospheric values on the unilluminated surface are negligible; on a thermal timescale of the convective envelope $\tau_{\rm ce}$ the star relaxes thermally according to the modified outer boundary conditions by adjusting R_2, T_0, and $L_{\rm nuc}$. Ritter (1994); Ritter et al. (2000) give an analytical estimate for the effect of irradiation on the thermal equilibrium values of low-mass MS stars. The effective temperature remains basically unchanged and the radius increases by about $(1-s)^{-0.1}$, i.e., $\leq 5\%$ for typical values of s.

For our numerical computations we compute $\dot{R}_2$ by solving the equations of stellar structure for the donor star. This will be described in more detail in Sect. 5.

2.6. Mass transfer cycles

Fig. 6 shows schematically how the feedback between mass transfer rate, irradiation, and thermal relaxation works: As soon as mass transfer starts, the accretion rate $\dot{M}_1$ and also the accretion luminosity $L_{\rm accr}$ increase. This enhances the irradiating flux $F_{\rm irr}$ which reduces the intrinsic luminosity $L_{\rm int}$. Thus, the thermal expansion rate $\dot{R}_2$ of the star is increased which in turn leads to an increasing mass transfer rate $-\dot{M}_2$.

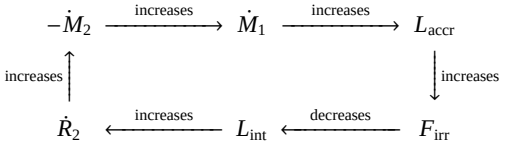

Figure 6. Schematic diagram of the irradiation feedback mechanism at turn on of mass transfer.

Yet, this feedback can not work forever because thermal relaxation saturates at last after about a Kelvin-Helmholtz timescale $\tau_{\rm KH}$. But before the star reaches a new equilibrium state, the expansion rate starts dropping and the mass transfer rate is reduced. Then the feedback works into the opposite direction: $\dot{M}_1$ and $L_{\rm accr}$ decrease and so does $F_{\rm irr}$. Therefore, $L_{\rm int}$ increases and the star starts to shrink. This reduces the mass transfer even more. In extreme cases the mass transfer even stops and the system appears as a detached system until the next cycle starts.

3. The analytical model

We will now derive an analytical model that describes the onset of mass transfer cycles. In principle, this has already been done by King et al. (1996) using a slightly different formalism. All expressions derived in section 3 and also 4 will be applied to the analytical model only and will not be used for the numerical computations.

3.1. The governing differential equations

The time evolution of the Roche radius $R_{\rm R,2}$ can be written as

$$\frac{{\rm d}\ln R_{\rm R,2}}{{\rm d}t} = \zeta_{\rm R}\frac{{\rm d}\ln M_2}{{\rm d}t} + 2\left(\frac{{\rm d}\ln J}{{\rm d}t}\right)_{\rm sys}, \tag{26}$$

where subscript $_{\rm sys}$ denotes the systemic angular momentum loss at constant total mass M (e.g., angular momentum loss by gravitational radiation) and

$$\zeta_{\rm R} = (1-\bar{\eta})(2\nu+1)\frac{q}{1+q} - 2(1-\bar{\eta}q) + (1+\bar{\eta}q)\frac{{\rm d}f_{\rm R}}{{\rm d}\ln q} \tag{27}$$

the mass radius exponent of the critical Roche radius (e.g., Ritter 1999)[3]. Angular momentum loss by CAML is taken into account by $\zeta_{\rm R}$, and the dimensionless Roche radius

$$f_{\rm R} = \frac{R_{\rm R,2}}{A} \tag{28}$$

is available in tabulated form (Mochnacki 1984).

The time evolution of the radius R_2 can be splitted into three terms: The adiabatic reaction at constant entropy and chemical composition, the thermal relaxation at constant chemical composition, and the nuclear evolution:

$$\frac{{\rm d}\ln R_2}{{\rm d}t} = \zeta_{\rm s}\frac{{\rm d}\ln M_2}{{\rm d}t} + \left(\frac{{\rm d}\ln R_2}{{\rm d}t}\right)_{\rm th} + \left(\frac{{\rm d}\ln R_2}{{\rm d}t}\right)_{\rm nuc} \tag{29}$$

with the adiabatic mass radius exponent $\zeta_{\rm s}$.

The time evolution of the equilibrium radius $R_{\rm e,2}$ of the unilluminated star is given by

$$\frac{{\rm d}\ln R_{\rm e,2}}{{\rm d}t} = \zeta_{\rm e}\frac{{\rm d}\ln M_2}{{\rm d}t} + \left(\frac{{\rm d}\ln R_{\rm e,2}}{{\rm d}t}\right)_{\rm nuc}, \tag{30}$$

where $\zeta_{\rm e}$ denotes the thermal equilibrium mass radius exponent (e.g., Webbink 1985).

With the timescale of nuclear evolution

$$\tau_{\rm nuc} = \left(\frac{{\rm d}\ln R_2}{{\rm d}t}\right)^{-1}_{\rm nuc} \approx \left(\frac{{\rm d}\ln R_{\rm e,2}}{{\rm d}t}\right)^{-1}_{\rm nuc}, \tag{31}$$

[3] In that paper q is defined as $\frac{M_1}{M_2}$, i.e., inverse of the definition here.

the timescale of systemic angular momentum loss

$$\tau_{\rm J} = -\left(\frac{{\rm d}\ln J}{{\rm d}t}\right)^{-1}_{\rm sys}, \tag{32}$$

and the timescale of thermal relaxation

$$\tau_{\rm th} = \left(\frac{{\rm d}\ln R_2}{{\rm d}t}\right)^{-1}_{\rm th} \tag{33}$$

we define the driving timescale for the mass loss by

$$\frac{1}{\tau_{\rm d}} = \frac{1}{\tau_{\rm nuc}} + \frac{2}{\tau_{\rm J}}, \tag{34}$$

and the driving timescale including the thermal relaxation by

$$\frac{1}{\tau'_{\rm d}} = \frac{1}{\tau_{\rm d}} + \frac{1}{\tau_{\rm th}}. \tag{35}$$

Using (26) and (29) and taking into account $R_2 \approx R_{\rm R,2}$ the time evolution of $\Delta R = R_2 - R_{\rm R,2}$ can be written as

$$\frac{\rm d}{{\rm d}t}\Delta R = (\zeta_{\rm s} - \zeta_{\rm R})\, R_2 \frac{\dot M_2}{M_2} + \frac{R_2}{\tau_{\rm th}} + \frac{R_2}{\tau_{\rm d}}. \tag{36}$$

Using (29) and (30) and assuming[4] $R_2 \approx R_{\rm e,2}$ the time evolution of

$$\Delta R_{\rm e} = R_2 - R_{\rm e,2} \tag{37}$$

can be written as

$$\frac{\rm d}{{\rm d}t}\Delta R_{\rm e} = (\zeta_{\rm s} - \zeta_{\rm e})\, R_2 \frac{\dot M_2}{M_2} + \frac{R_2}{\tau_{\rm th}}. \tag{38}$$

(36) and (38) are the governing differential equations and are analogous to Eqs. [11] and [12] of King et al. (1996).

3.2. The stationary state

One can easily see from (3) that the mass transfer rate is stationary if and only if ΔR is constant. Setting the left-hand side of (36) to zero yields the stationary mass transfer rate

$$\overline{\dot M}_2 = -\frac{M_2}{\zeta_{\rm s} - \zeta_{\rm R}}\left(\frac{1}{\tau_{\rm th}} + \frac{1}{\tau_{\rm d}}\right) = -\frac{1}{\zeta_{\rm s} - \zeta_{\rm R}}\frac{M_2}{\tau'_{\rm d}}. \tag{39}$$

Additionally, the thermal relaxation

$$K := \frac{R_2}{\tau_{\rm th}} \tag{40}$$

is stationary if $\Delta R_{\rm e}$ is also constant. Setting the left-hand side of (38) to zero and inserting (39) yields for the stationary thermal relaxation $\overline{K}$:

$$\frac{\overline{K}}{R_2} = \frac{1}{\overline{\tau}_{\rm th}} = \frac{\zeta_{\rm s} - \zeta_{\rm e}}{\zeta_{\rm e} - \zeta_{\rm R}}\frac{1}{\tau_{\rm d}}. \tag{41}$$

From (39) and (41) it can be seen immediatly that the stationary solution is unique if there is any at all because $\overline{\dot M}_2$ and $\overline{K}$ depend on the system parameters $\zeta_{\rm s}$, $\zeta_{\rm e}$, $\zeta_{\rm R}$, and $\tau_{\rm d}$ only. By inserting (41) into (39) the timescale of mass transfer can be expressed by the driving timescale:

$$\tau_{\rm M} := -\frac{M_2}{\overline{\dot M}_2} = (\zeta_{\rm e} - \zeta_{\rm R})\,\tau_{\rm d}. \tag{42}$$

[4] This assumption is not necessarily fulfilled, especially for giants, but it simplifies the following equations and does not affect the results significantly.

4. Linear stability analysis

To determine the conditions for stability of the stationary solution we perform a linear stability analysis (see, e.g., Guckenheimer & Holmes 1983) on the vector field

$$\boldsymbol{F}\begin{pmatrix}\Delta R\\ \Delta R_{\rm e}\end{pmatrix} = \begin{pmatrix}(\zeta_{\rm s} - \zeta_{\rm R})\, R_2 \frac{\dot M_2}{M_2} + K + \frac{R_2}{\tau_{\rm d}}\\ (\zeta_{\rm s} - \zeta_{\rm e})\, R_2 \frac{\dot M_2}{M_2} + K\end{pmatrix} \tag{43}$$

around the stationary solution $\left(\overline{\Delta R}, \overline{\Delta R_{\rm e}}\right)$, which is a fixed point of $\boldsymbol{F}$, i.e., $\boldsymbol{F}\left(\overline{\Delta R}, \overline{\Delta R_{\rm e}}\right) = \boldsymbol{0}$.

4.1. The necessary criterion

According to the theorem of Hartmann-Grobmann a fixed point $\boldsymbol{x}$ of a vector field $\boldsymbol{F}$ is stable, if all eigenvalues of the Jacobi matrix $\boldsymbol{DF}$ of $\boldsymbol{F}$ at $\boldsymbol{x}$ have a negative real part, and $\boldsymbol{x}$ is unstable if at least one eigenvalue has a positive real part.

Using (3) and neglecting the derivatives of $\tau_{\rm nuc}$ and R_2, which is reasonable for $\tau_{\rm nuc}$, $\tau_{\rm M} \gg \tau_{\rm KH}$, and neglecting also the derivatives of $\tau_{\rm J}$ we get

$$\boldsymbol{DF}\begin{pmatrix}\overline{\Delta R}\\ \overline{\Delta R_{\rm e}}\end{pmatrix} = \begin{pmatrix}(\zeta_{\rm s} - \zeta_{\rm R})\frac{R_2}{H_{\rm P}}\frac{\overline{\dot M}_2}{M_2} + \frac{\partial K}{\partial \Delta R} & \frac{\partial K}{\partial \Delta R_{\rm e}}\\ (\zeta_{\rm s} - \zeta_{\rm e})\frac{R_2}{H_{\rm P}}\frac{\overline{\dot M}_2}{M_2} + \frac{\partial K}{\partial \Delta R} & \frac{\partial K}{\partial \Delta R_{\rm e}}\end{pmatrix} \tag{44}$$

at the fixed point.

$\boldsymbol{DF}$ has the eigenvalues

$$\lambda_{1,2} = \frac{1}{2}{\rm tr}\,\boldsymbol{DF} \pm \sqrt{\frac{1}{4}{\rm tr}^2\,\boldsymbol{DF} - \det \boldsymbol{DF}}. \tag{45}$$

Since $\boldsymbol{DF}$ is a real matrix, the necessary condition for ${\rm Re}\,\lambda_{1,2} < 0$ is

$${\rm tr}\,\boldsymbol{DF} = (\zeta_{\rm s} - \zeta_{\rm R})\frac{R_2}{H_{\rm P}}\overline{\dot M}_2 + \frac{\partial K}{\partial \Delta R} + \frac{\partial K}{\partial \Delta R_{\rm e}} < 0. \tag{46}$$

If the thermal relaxation K is neglected, Eq. (46) is equivalent to

$$\zeta_{\rm s} - \zeta_{\rm R} > 0, \tag{47}$$

the well-known criterion for dynamical stability (e.g., Webbink 1985). Since only dynamically stable systems can undergo long phases of mass transfer, we consider only such systems.

The first term in (46) reflects the adiabatic reaction of the star and its Roche radius on mass loss. For dynamically stable systems this term is negative and therefore it contributes to the stabilization of the fixed point. The third term in (46) tells how thermal relaxation changes with the radius of the star compared to its equilibrium radius. A negative value means that the larger (smaller) R_2, the stronger the thermal relaxation that decreases (increases) the radius to its (irradiation-dependend) equilibrium value. Therefore,

$$\frac{\partial K}{\partial \Delta R_{\rm e}} < 0 \tag{48}$$

is a reasonable assumption about the thermal relaxation K. Thus, the necessary criterion for stability (46) can only be violated if

$$\frac{\partial K}{\partial \Delta R} > 0. \tag{49}$$

This means that an increasing (decreasing) ΔR and therefore an increasing (decreasing) mass transfer rate tends to enhance thermal relaxation which drives the expansion (contraction) of the star even more. Exactly this kind of feedback is caused by irradiation. The question is now whether this feedback can be strong enough to overwhelm the stabilizing terms in (46).

4.2. The sufficient criterion

The sufficient criterion for $\mathrm{Re}\,\lambda_{1,2} < 0$ is that the absolute value of the real part of the square root in (45) is less than the absolute value of $\frac{1}{2}\mathrm{tr}\,\boldsymbol{DF}$, otherwise at least one eigenvalue has a positive real part. Using (44) it can be shown that this is equivalent to $\det \boldsymbol{DF} > 0$ which is equivalent to

$$\zeta_\mathrm{e} - \zeta_\mathrm{R} > 0. \tag{50}$$

This is the well-known criterion for thermal stability (e.g., Webbink 1985). Only thermally stable systems can have stable stationary solutions since thermally unstable systems transfer mass on a thermal timescale. As a consequence, the thermal relaxation K can never reach a stationary value. Therefore, we consider only systems that are thermally stable.

4.3. The onset of instability

There are different possibilities for the dynamics of the system nearby the fixed point depending on $\mathrm{tr}\,\boldsymbol{DF}$ and $\det \boldsymbol{DF}$ if (47) and (50) are fulfilled:

- $\mathrm{tr}\,\boldsymbol{DF} \le -2\sqrt{\det \boldsymbol{DF}}$: We have $\mathrm{tr}^2\,\boldsymbol{DF} \ge 4\det \boldsymbol{DF}$ so that the eigenvalues $\lambda_{1,2}$ in (45) are real and negative. All solutions near the fixed point converge directly to the fixed point without any oscillation.
- $-2\sqrt{\det \boldsymbol{DF}} < \mathrm{tr}\,\boldsymbol{DF} < 0$: We have $\mathrm{tr}^2\,\boldsymbol{DF} < 4\det \boldsymbol{DF}$ so that the square root in (45) is imaginary. The eigenvalues can be written as $\lambda_{1,2} = -\lambda \pm \mathrm{i}\omega$ with $\lambda, \omega > 0$. All solutions near the fixed point spiral in.
- $\mathrm{tr}\,\boldsymbol{DF} = 0$: The eigenvalues $\lambda_{1,2} = \pm\mathrm{i}\omega$ are imaginary. The system undergoes a Hopf bifurcation, when the fixed point, that is stable for $\mathrm{tr}\,\boldsymbol{DF} < 0$, becomes unstable, and a stable limit circle arises for $\mathrm{tr}\,\boldsymbol{DF} > 0$. In principle, this could be proved mathematically in terms of normal form theory (Guckenheimer & Holmes 1983, theorem 3.4.2 and eq. 3.4.11) but it requires explicit knowledge of $\dot{M}_2(\Delta R)$ and $K(\Delta R, \Delta R_\mathrm{e})$.
- $0 < \mathrm{tr}\,\boldsymbol{DF} < 2\sqrt{\det \boldsymbol{DF}}$: We have $\mathrm{tr}^2\,\boldsymbol{DF} < 4\det \boldsymbol{DF}$ so that the square root in (45) is imaginary. The eigenvalues can be written as $\lambda_{1,2} = +\lambda \pm \mathrm{i}\omega$ with $\lambda, \omega > 0$. All solutions near the fixed point spiral out and converge to the limit cycle sketched in Sect. 2.6.
- $2\sqrt{\det \boldsymbol{DF}} \le \mathrm{tr}\,\boldsymbol{DF}$: We have $\mathrm{tr}^2\,\boldsymbol{DF} \ge 4\det \boldsymbol{DF}$ so that the eigenvalues $\lambda_{1,2}$ in (45) are real and positive. All solutions near the fixed point diverge directly without any oscillation and converge to the limit cycle.

4.4. The irradiation feedback

Since K depends on ΔR via the intrinsic luminosity L_int, the derivative $\frac{\partial K}{\partial \Delta R}$ can be written as

$$\frac{\partial K}{\partial \Delta R} = \left(\frac{\mathrm{d}K}{\mathrm{d}L_\mathrm{int}}\right)_{\Delta R_\mathrm{e}} \left(\frac{\mathrm{d}L_\mathrm{int}}{\mathrm{d}\Delta R}\right)_{\Delta R_\mathrm{e}}. \tag{51}$$

L_int does not depend on ΔR directly but indirectly via s. Additionally, R_2 and T_0 do not depend on $\dot{M}_2$. Therefore we can write:

$$\left(\frac{\mathrm{d}L_\mathrm{int}}{\mathrm{d}\Delta R}\right)_{\Delta R_\mathrm{e}} = \left(\frac{\mathrm{d}L_\mathrm{int}}{\mathrm{d}s}\right)_{R_2,T_0} \frac{\mathrm{d}s}{\mathrm{d}\dot{M}_2} \frac{\mathrm{d}\dot{M}_2}{\mathrm{d}\Delta R}. \tag{52}$$

From (17) we obtain

$$\left(\frac{\mathrm{d}L_\mathrm{int}}{\mathrm{d}s}\right)_{R_2,T_0} = -4\pi\sigma T_0^4 R_2^2 \tag{53}$$

and from (3)

$$\frac{\mathrm{d}\dot{M}_2}{\mathrm{d}\Delta R} = \frac{\dot{M}_2}{H_\mathrm{P}}. \tag{54}$$

With the definition of

$$s' := \dot{M}_2 \frac{\mathrm{d}s}{\mathrm{d}\dot{M}_2} = \frac{\mathrm{d}s}{\mathrm{d}\ln\left(-\dot{M}_2\right)} > 0, \tag{55}$$

which is a measure for how strongly the blocking of the intrinsic luminosity changes with $\dot{M}_2$ (or f_irr), Eqs. (51)-(55) give

$$\frac{\partial K}{\partial \Delta R} = -\frac{4\pi\sigma T_0^4 R_2^2}{H_\mathrm{P}} \left(\frac{\mathrm{d}K}{\mathrm{d}L_\mathrm{int}}\right)_{\Delta R_\mathrm{e}} s'. \tag{56}$$

Using (5) and (24) in (19) leads to

$$s'_\mathrm{ps} = -\frac{1}{2}\int_0^{\vartheta_\mathrm{max}} \frac{\mathrm{d}f_\mathrm{int}}{\mathrm{d}f_\mathrm{irr}} \langle f_\mathrm{irr}\rangle\, h(\vartheta)\, \sin\vartheta\, \mathrm{d}\vartheta \tag{57}$$

for the point source model while (23) leads to

$$s'_\mathrm{cf} = -\frac{1}{2} s_\mathrm{max} \frac{\mathrm{d}f_\mathrm{int}}{\mathrm{d}f_\mathrm{irr}} \langle f_\mathrm{irr}\rangle \tag{58}$$

for the constant flux model. Figs. 7 and 8 show s'_cf and s'_ps for different stellar models and also for a simple prescription for s that was used by King et al. (1995, 1997):

$$s_k = s_\mathrm{max} \tanh\left(k\langle f_\mathrm{irr}\rangle\right). \tag{59}$$

k is a free parameter that defines the position of the maximum of

$$s'_k = s_\mathrm{max} \frac{k\langle f_\mathrm{irr}\rangle}{\cosh^2\left(k\langle f_\mathrm{irr}\rangle\right)}. \tag{60}$$

As can be easily seen from (58) and also from (57) or (60), s' vanishes for $\langle f_\mathrm{irr}\rangle \to 0$ (no irradiation means no feedback) and for $\langle f_\mathrm{irr}\rangle \to \infty$ (strong irradiation means saturation, i.e., $s = s_\mathrm{max}$ is constant).

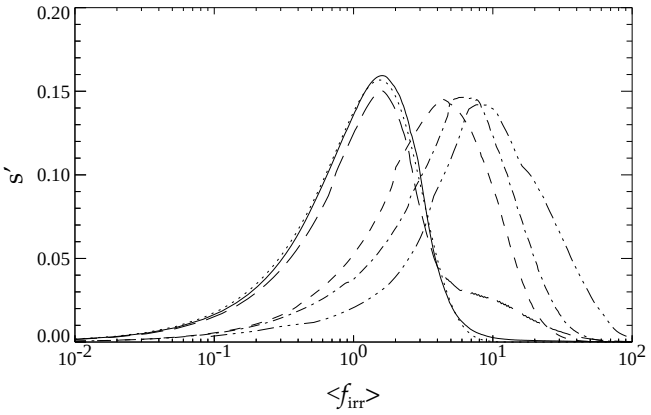

Figure 7. $s'_{\rm cf}$ (Eq. (58)) for stellar models no. 1-4 and 6 of table 1 (solid, long-dashed, short-dashed, dash-dotted and dot-dash-dotted line, respectively) and also s'_k for $k = 1$ (Eq. (60), dotted line).

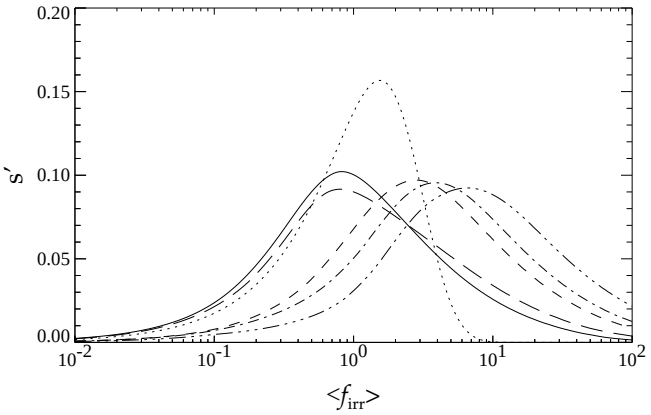

Figure 8. $s'_{\rm ps}$ (Eq. (57)) for the same stellar models as in Fig. 7. For comparison of the point source with the constant flux model also s'_k for $k = 1$ (Eq. (60)) is shown.

4.5. The bipolytrope model

In terms of a bipolytrope model the thermal relaxation K can be expressed explicitely (Kolb & Ritter 1992, eq. 32). If the star is either fully convective or the nuclear luminosity of the radiative core is identical to the total luminosity of the core, which is the case in the stationary (i.e., quasi-equilibrium) state, then the thermal relaxation can be expressed as

$$\frac{K}{R_2} = \left(\frac{{\rm d}\ln R_2}{{\rm d}t}\right)_{\rm th} = -\mathcal{F}\frac{R_2\,(L_{\rm int} - L_{\rm nuc})}{\Gamma M_2^2}. \tag{61}$$

$\mathcal{F}$ is given by Eq. [47] of King et al. (1996) for chemically homogeneous stars and can be approximated by

$$\mathcal{F} \approx \frac{7}{3}\frac{M_2}{M_{\rm ce}}, \tag{62}$$

where $M_{\rm ce}$ denotes the mass of the convective envelope (King et al. 1996; Ritter et al. 2000).

The only quantity in (61) which depends on $L_{\rm int}$ is $L_{\rm int}$ itself:

$$\left(\frac{{\rm d}K}{{\rm d}L_{\rm int}}\right)_{\Delta R_{\rm e}} = R_2\left(\frac{\rm d}{{\rm d}L_{\rm int}}\frac{K}{R_2}\right) = -\frac{\mathcal{F}R_2^2}{\Gamma M_2^2}. \tag{63}$$

Inserting this into (56) gives

$$\frac{\partial K}{\partial \Delta R} = \mathcal{F}\frac{4\pi\sigma T_0^4 R_2^4}{H_{\rm P}\Gamma M_2^2}s'. \tag{64}$$

This can be expressed by quantities of the unilluminated star: In terms of the Kelvin-Helmholtz timescale

$$\tau_{\rm KH} = \frac{\Gamma M_2^2}{R_{\rm e,2}L_0} \tag{65}$$

the corresponding timescale of the convective envelope is given by

$$\tau_{\rm ce} = \frac{\tau_{\rm KH}}{\mathcal{F}} \sim \frac{3}{7}\frac{M_{\rm ce}}{M_2}\tau_{\rm KH}. \tag{66}$$

Using (17) and (66) Eq. (64) can be written as

$$\frac{\partial K}{\partial \Delta R} = \frac{R_2}{H_{\rm P}}\frac{s'}{\tau_{\rm ce}}\left(\frac{R_{\rm s}}{R_e}\right)^3 \tag{67}$$

and is analogous to Eq. [44], respectively [59] of King et al. (1996). Alternatively, (64) can also be expressed by quantities of the illuminated star:

$$\frac{\partial K}{\partial \Delta R} = \frac{R_2}{H_{\rm P}}\frac{s'}{1-s}\frac{1}{\tau_{\rm ce,s}}. \tag{68}$$

In this case the (irradiation-dependent) timescale of the convective envelope

$$\tau_{\rm ce,s} = \frac{\tau_{\rm KH,s}}{\mathcal{F}} \tag{69}$$

is defined via the Kelvin-Helmholtz timescale

$$\tau_{\rm KH,s} = \frac{\Gamma M_2^2}{R_2 L_{\rm int}} \tag{70}$$

of the illuminated star taking into account that it can radiate only through its unilluminated surface with $L_{\rm int}$ given by (17).

4.6. The homology model

The energy generation rate from hydrogen burning can be approximated by a simple power law of density ρ and temperature T:

$$\varepsilon_{\rm nuc} \sim \rho T^n. \tag{71}$$

For low-mass MS stars, which are considered here, the pp-chain gives n = 5 – 6 (see, e.g., Kippenhahn & Weigert 1990). By using homology relations we obtain

$$L_{\rm nuc} = L_0\left(\frac{R_2}{R_{\rm e,2}}\right)^{-(n+3)} \tag{72}$$

for main sequence stars. Since for giants the nuclear luminosity does not depend on the stellar radius, the following expressions also apply to giants if we set $n = -3$.

Inserting (17) and (72) into (61) gives:

$$K = -\frac{\mathcal{F}}{\Gamma M_2^2}\left[4\pi\,(1-s)\,T_0^4 R_2^4 - L_0 R_{\mathrm{e},2}^2\left(\frac{R_2}{R_{\mathrm{e},2}}\right)^{-(n+1)}\right]. \tag{73}$$

The equilibrium radius $R_{\mathrm{e},2}$ of the unilluminated star neither depends on ΔR nor on ΔR_{e}. This means

$$\frac{\partial R_2}{\partial \Delta R_{\mathrm{e}}} = \frac{\partial}{\partial \Delta R_{\mathrm{e}}}\left(R_{\mathrm{e},2} + \Delta R_{\mathrm{e}}\right) = 1. \tag{74}$$

Therefore, the derivative of K with respect to ΔR_{e} yields:

$$\frac{\partial K}{\partial \Delta R_{\mathrm{e}}} = -\frac{\mathcal{F} L_0 R_{\mathrm{e},2}\left[4\,(1-s)\left(\frac{R_2}{R_{\mathrm{e},2}}\right)^3 + (n+1)\left(\frac{R_2}{R_{\mathrm{e},2}}\right)^{-(n+2)}\right]}{\Gamma M_2^2}. \tag{75}$$

This can be written in quantities of the unilluminated star:

$$\frac{\partial K}{\partial \Delta R_{\mathrm{e}}} = -\frac{\left[4\,(1-s)\left(\frac{R_2}{R_{\mathrm{e},2}}\right)^3 + (n+1)\left(\frac{R_2}{R_{\mathrm{e},2}}\right)^{-(n+2)}\right]}{\tau_{\mathrm{ce}}}. \tag{76}$$

This result is analogous to Eq. [43] of King et al. (1996) who have computed the derivative[5] of $\frac{K}{R_2}$ while we use the derivative of K. This leads to different values for the powers of $\frac{R_2}{R_{\mathrm{e},2}}$ in their Eq. [43] compared to our Eq. (76): 3 and $n+2$ versus 4 and $n+1$. The origin of this difference is the approximate transition from linear to logarithmic derivatives in Eq. [2] of King et al. (1996).

Alternatively, (75) can also be expressed in quantities of the illuminated star. Using (69), (70), (72) and $L_{\mathrm{int}} = L_{\mathrm{nuc}}$ in the (irradiation dependend) equilibrium state we get the more compact expression:

$$\frac{\partial K}{\partial \Delta R_{\mathrm{e}}} = -\frac{n+5}{\tau_{\mathrm{ce,s}}}. \tag{77}$$

Finally, we can insert (68) and (77) into the necessary criterion for stability (46) and get

$$-\frac{\mathrm{d}\ln(1-s)}{\mathrm{d}\ln\left(-\dot{M}\right)} = \frac{s'}{1-s} < \frac{\tau_{\mathrm{ce,s}}}{\tau'_{\mathrm{d}}} + \frac{H_{\mathrm{P}}}{R_2}\,(n+5) \tag{78}$$

in quantities of the illuminated star. By inserting (67) and (76) into (46) we get the equivalent result in quantities of the unilluminated star:

$$s' < \frac{\tau_{\mathrm{ce}}}{\tau'_{\mathrm{d}}} + \frac{H_{\mathrm{P}}}{R_2}\delta, \tag{79}$$

where δ is given by

$$\delta = 4\,(1-s)\left(\frac{R_2}{R_{\mathrm{e},2}}\right)^3 + (n+1)\left(\frac{R_2}{R_{\mathrm{e},2}}\right)^{-(n+3)} \sim n+5. \tag{80}$$

If s' is less than the ratio of τ_{ce} and τ'_{d} plus a term of the order of several $\frac{H_{\mathrm{P}}}{R_2}$, then the stationary mass transfer rate is stable. Otherwise it is unstable and mass transfer cycles occur.

[5] In that paper K is defined as $\left(\frac{\mathrm{d}\ln R}{\mathrm{d}t}\right)_{\mathrm{th}}^{-1}$.

4.7. Predictions of the analytical model

Taking (22), eliminating A by (28), $\overline{\dot{M}}_2$ by (39) and using the driving timescale τ'_{d} including the thermal relaxation from (35) we obtain

$$\frac{1}{\tau'_{\mathrm{d}}} = \frac{\zeta_{\mathrm{s}} - \zeta_{\mathrm{R}}}{\alpha\eta} 4\pi\sigma T_0^4 \frac{R_{\mathrm{R},2}^2 R_1}{f_{\mathrm{R}}^2 \Gamma M_1 M_2}\,\langle f_{\mathrm{irr}}\rangle\,. \tag{81}$$

With (66) the ratio of τ_{ce} and τ'_{d} can be written as

$$\frac{\tau_{\mathrm{ce}}}{\tau'_{\mathrm{d}}} = \frac{\zeta_{\mathrm{s}} - \zeta_{\mathrm{R}}}{\alpha\eta\mathcal{F}} \frac{M_2 R_1 R_{\mathrm{R},2}^2}{M_1 R_2^3 f_{\mathrm{R}}^2}\,\langle f_{\mathrm{irr}}\rangle\,. \tag{82}$$

This result can be approximated by using (62), $R_2 \approx R_{\mathrm{R},2}$ and the approximation (Paczyński 1971)

$$f_{\mathrm{R}}(q) \approx \left(\frac{8}{3^4}\right)^{\frac{1}{3}}\left(\frac{q}{q+1}\right)^{\frac{1}{3}} \tag{83}$$

as

$$\frac{\tau_{\mathrm{ce}}}{\tau'_{\mathrm{d}}} \approx \frac{3}{7}\left(\frac{3^4}{8}\right)^{\frac{2}{3}} \frac{\zeta_{\mathrm{s}} - \zeta_{\mathrm{R}}}{\alpha\eta}\,(1+q)^{\frac{2}{3}}\,q^{\frac{1}{3}}\,\frac{M_{\mathrm{ce}}}{M_2}\,\frac{R_1}{R_2}\,\langle f_{\mathrm{irr}}\rangle\,. \tag{84}$$

This is a function of $\langle f_{\mathrm{irr}}\rangle$ and its slope basically depends only on $\alpha\eta$, the relative mass of the convective envelope $\frac{M_{\mathrm{ce}}}{M_2}$ and the ratio of the radii of both stars $\frac{R_1}{R_2}$. The other factors are of order unity for typical system parameters.

For the moment we neglect the last term of order of several $\frac{H_{\mathrm{P}}}{R_2}$ in criterion (79) as King et al. (1996) did. To get mass transfer cycles the blocking of the intrinsic flux (s') as a reaction upon an enhanced mass transfer rate must increase faster than the convective envelope can relax thermally (τ_{ce}) compared to the driving time scale of the mass loss (τ'_{d}). Therefore, systems are the more susceptible to the onset of mass transfer cycles, the smaller the timescale of the convective envelope τ_{ce} and the larger the driving timescale $\tau_{\mathrm{d}} \sim \tau'_{\mathrm{d}}$ is.

Accordingly, main sequence stars with thin outer convection zones ($M_2 \sim 1\,M_\odot$) have been supposed to be most susceptible (King et al. 1996; Ritter et al. 2000). Also systems driven by the longest possible timescale, i.e., the timescale of angular momentum loss by gravitational radiation, have been supposed to be more susceptible than other systems. But there are basically no systems except, e.g., low-mass CVs in or below the period gap that are driven mainly by gravitational braking. Higher mass systems are believed to be driven mainly by magnetic breaking. For a high braking rate, e.g., according to Verbunt & Zwaan (1981), CVs with unevolved main sequence stars become unsusceptible to the irradiation instability except for the most massive systems because τ_{d} becomes too small in comparison to τ_{ce} (Ritter et al. 1995, 1996, 2000). For giants magnetic braking is believed to be ineffective and τ_{ce} is small compared to $\tau_{\mathrm{d}} \approx \tau_{\mathrm{nuc}}$. Therefore, such systems and also CVs with highly evolved MS stars, which have a short τ_{ce}, have been supposed to be a priori more susceptible to the irradiation instability than CVs with unevolved MS stars (King et al. 1997).

But the last term of order of several $\frac{H_{\mathrm{P}}}{R_2}$ in (79) can be neglected only if

$$\frac{H_{\mathrm{P}}}{R_2} \ll \frac{\tau_{\mathrm{ce}}}{\tau_{\mathrm{d}}}. \tag{85}$$

As soon as τ_{ce} gets small (as for main sequence stars of $\sim 1 M_\odot$) or $\frac{H_P}{R_2}$ is no longer very small (as for giants), this term must be taken into account. Obviously, the range of $\langle f_{irr} \rangle$ in which

$$s' > \frac{H_P}{R_2}\delta \tag{86}$$

can be fulfilled, is an interval $[\langle f_{irr,min} \rangle, \langle f_{irr,max} \rangle]$ because s' vanishes for $\langle f_{irr} \rangle \to 0$ and $\langle f_{irr} \rangle \to \infty$. Thus, mass transfer cycles can only occur in a limited range of $\langle f_{irr} \rangle$. This range, that is predicted by the analytical model, has to be checked by numerical computations with full stellar models.

In this section we have derived a more concise and, in some sense, more general, expression (78), respectively (79) for the onset of instability than the corresponding Eq. [45], respectively [60] of King et al. (1996). We have also provided an explicit formula (84) for $\frac{\tau_{ce}}{\tau'_d}$ which we will use in Sect. 6 to discuss our numerical results. An important result is that the additional term of several $\frac{H_P}{R_2}$ in (79) provides an upper limit for τ_d, i.e., a lower limit for $-\overline{\dot{M}_2}$. Hence, for a sufficiently low secular mass transfer rate every system becomes stable. We will show in Sect. 6.1.3 that this limit can become important for CVs with giant donors.

5. The binary evolutionary code

We use the stellar evolutionary code of Schlattl et al. (1997); Schlattl (1999) which goes back to the code of Kippenhahn et al. (1967). The code uses a special grid point algorithm (Wagenhuber & Weiss 1994), nuclear reaction rates of Caughlan et al. (1985); Adelberger et al. (1998), the mixing length theory of Böhm-Vitense (1958); Cox & Giuli (1968), the OPAL opacities (Iglesias & Rogers 1996), and for the outer layers opacities by Alexander & Ferguson (1994) and additional data from P. H. Hauschildt and J. W. Ferguson (priv. comm.). In order to avoid numerical instabilities in calculating mass transfer it was necessary to implement an equation of state which is smooth in the independent variables P, T, and chemical composition over the whole range of application. In practice, we use the equation of state of Saumon et al. (1995) with data provided by I. Baraffe (priv. comm.), and particularly the equation of state of Pols et al. (1995). Furthermore, we developed an implicit algorithm for the treatment of mass transfer similar to the method described by Benvenuto & de Vito (2003). For more details about our code see Büning (2003). For determining f_{int} (f_{irr}) we use results given by Hameury & Ritter (1997) and additional data from J.-M. Hameury (priv. comm.).

6. Numerical results

To destabilize the stationary mass transfer the ratio of τ_{ce} and τ'_d has to be sufficiently small, at least less than the maximum of s' which is ~ 0.1. As can be seen from (84), especially for realistic values of $\alpha\eta < 1$ the ratio $\frac{R_1}{R_2}$ has to be sufficiently small for typical system parameters which is basically the case for compact binaries only. Since the system has to be dynamically and thermally stable and since the donor star has to maintain a deep convective envelope, essentially only CVs and LMXBs are eligible.

Model No.	$M_1/M_\odot$	q	$\overline{\eta}$	ν	ζ_R	α
1	0.8	$\frac{5}{8}$	1	-	-0.35	0.3
2	1.2	$\frac{5}{12}$	0	-	-1.20	0.3
3	0.8	$\frac{5}{8}$	0	q	-0.89	0.3
4	0.8	$\frac{5}{8}$	0	q	-0.89	0.1

Table 2. System parameters of CVs containing an $0.5\,M_\odot$ donor as shown in Fig. 9.

6.1. Cataclysmic variables

6.1.1. Unevolved MS donors

Exemplarily for a wide range of CVs with unevolved donor stars Fig. 9 shows the left-hand and also the right-hand side of (79), namely s' and

$$f := \delta\frac{H_P}{R_2} + \frac{\tau_{ce}}{\tau'_d} \tag{87}$$

for a CV with an $0.8\,M_\odot$ white dwarf and an unevolved $0.5\,M_\odot$ MS secondary using system parameters listed in table 2. Low-mass MS stars have $\frac{H_P}{R_2} \sim 10^{-4}$ and $\delta \sim n + 5 \approx 10$. This leads to an almost constant contribution $\sim 10^{-3}$ to f while $\frac{\tau_{ce}}{\tau'_d}$ is almost linear in $\langle f_{irr} \rangle$. The most significant uncertainty in the values of f is due to the undetermined value of α (short-dashed vs. dash-dotted line in Fig. 9) while the influence of q (long-dashed vs. dash-dotted line) is negligible. Only $\overline{\eta}$ (dot-dash-dotted vs. dash-dotted line) has a noticable influence on f in this case since $\zeta_s - \zeta_R$ is much smaller in the conservative case. Systems with non-conservative mass transfer ($\overline{\eta} < 1$ and $\nu = q$) are systematically more stable than systems with conservative mass transfer ($\overline{\eta} = 1$). In the following discussion we will restrict ourselves to $\eta = 1$ and $\overline{\eta} = 0$ since this case is more realistic than $\overline{\eta} = 1$ (Hameury et al. 1989; Prialnik & Kovetz 1995). In general, the amplitude of the mass transfer cycles increases with the difference between s' and f for any given $\langle f_{irr} \rangle$.

As can be seen from Fig. 9, CVs with unevolved donors are the more stable, the smaller the irradiation efficiency α is. Such systems can undergo mass transfer cycles if $\alpha \gtrsim 0.1$. For, e.g., $\alpha = 0.3$ the "island of instability", which is defined by $s' > f$, ranges from $\langle f_{irr} \rangle \approx 5 \cdot 10^{-3}$ to $\langle f_{irr} \rangle \approx 2$. Using (84) is it possible to compute the corresponding ratio for τ_{ce} and τ'_d:

$$1.5 \cdot 10^{-4} \lesssim \frac{\tau_{ce}}{\tau'_d} \lesssim 7 \cdot 10^{-2}. \tag{88}$$

The timescale ratio must be within this range to destabilize the stationary mass transfer. With

$$\tau'_d = \frac{\zeta_e - \zeta_R}{\zeta_s - \zeta_R}\tau_d, \tag{89}$$

which can be obtained from (35) and (41), and $\tau_{ce} \sim 4.5 \cdot 10^7$ yr for an unevolved $0.5\,M_\odot$ MS star, we obtain a condition for the driving timescale τ_d:

$$3 \cdot 10^8\,\mathrm{yr} \lesssim \tau_d \lesssim 10^{11}\mathrm{yr}. \tag{90}$$

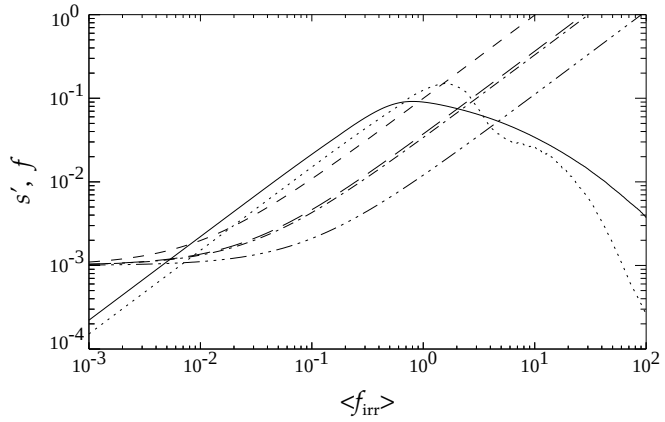

Figure 9. s' for a CV with an unevolved 0.5 $M_\odot$ MS star (no. 2 of table 1) and an 0.8 $M_\odot$ white dwarf for the point source and the constant flux model (solid and dotted line). s' is compared to f for models 1 − 4 listed in table 2 (dot-dash-dotted, long-dashed, dash-dotted and short-dashed line, respectively). The mass transfer is unstable and undergoes cycles if $s' > f$ which is only the case in a certain interval $[\langle f_{\rm irr,min}\rangle, \langle f_{\rm irr,max}\rangle]$ whose limits depend on α. Otherwise, the system is stable.

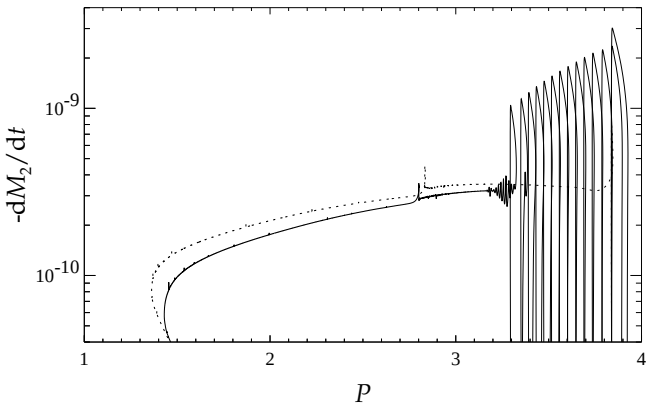

Figure 10. Mass transfer rate $-\dot{M}_2$ [$M_\odot$/yr] from a slightly evolved 0.5 $M_\odot$ MS star with an age of $\sim 10^{10}$ yr and $X_{\rm c} \approx 0.62$ onto an 0.8 $M_\odot$ white dwarf for the point source model as function of orbital period P [hr]. System parameters: $\overline{\eta} = 0$, $\nu = q$, $\alpha = 0.3$, and $\dot{J} = 5\dot{J}_{\rm grav}$ (solid line). The dotted line shows the mass transfer rate for the same system without irradiation feedback. Both computations have been stopped beyond the minimum period at $M_2 = 0.04\,M_\odot$.

If the evolution of the system is driven by gravitational braking only, i.e., $\tau_{\rm d} = \frac{\tau_{\rm J}}{2} \approx 4 \cdot 10^9$ yr, then the system must undergo mass transfer cycles. Gravitational braking provides a physical upper limit for the driving timescale. Since the lower limit in (90) is given by about $\frac{1}{10}$ of the gravitational braking timescale, we can expect the occurrence of the irradiation instability between $\dot{J} = \dot{J}_{\rm grav}$ and $\dot{J} \approx 10\dot{J}_{\rm grav}$ which is roughly confirmed by our numerical models.

Fig. 10 shows a CV evolution for initial parameters of model no. 3 of table 2 using the point source model and an ad hoc braking rate of $\dot{J} = 5\dot{J}_{\rm grav}$. The donor, a slightly evolved MS star, fills its Roche lobe at an orbital period of about 4 hr and starts to transfer mass undergoing cycles. At about 3.2 hr the system leaves the "island of instability" and becomes stable. The small spike in the mass transfer rate at about 2.8 hr is caused by the star becoming fully convective. For gravitational braking only as shown in Fig. 11 the phase of mass transfer cycles does not end until the system is in the middle of the period gap. The transition, when the star becomes fully convective, coincides with a drop in the peak mass transfer rate in this case.

The secular mass transfer rate is lower when taking irradiation into account (dotted versus solid line in Figs. 10 and 11) since the irradiated star has a systematically larger radius. As a consequence, the minimum period increases, in the case of pure gravitational braking by up to 2 minutes, depending on α. This is of the same order as the correction which is caused by geometrical distortion of the mass losing star by the Roche potential (Renvoizé et al. 2002), and this is still not sufficient to explain the observed orbital minimum period of $\sim$ 78 min (Ritter & Kolb 2003) if only gravitational braking is taken into account.

Fig. 12 shows the phase of mass transfer cycles as function of time for the same system as in Fig. 10. Since the eigenvalues

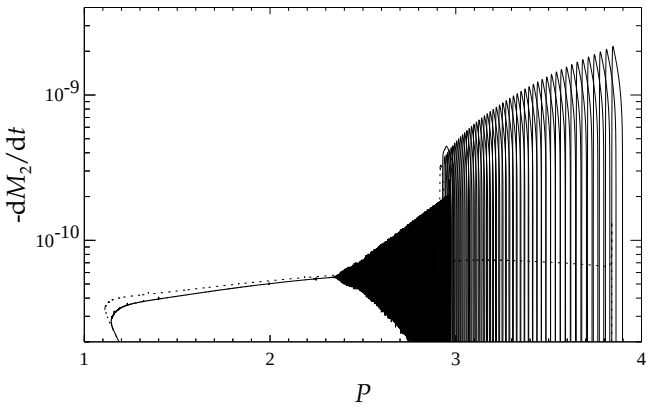

Figure 11. Same as Fig. 10 but for gravitational braking only.

at the fixed point are of the form $\lambda \pm {\rm i}\omega$, the frequency ω of the small amplitude oscillations at the end of the unstable phase can be computed from linear stability analysis using (44) and (77):

$$\omega = \sqrt{\det \boldsymbol{DF}} \approx \sqrt{\frac{R_2}{H_{\rm P}} \frac{1}{\tau'_{\rm d}} \frac{\delta}{\tau_{\rm ce}}}. \tag{91}$$

For the system considered we have $\frac{H_{\rm P}}{R_2} \approx 10^{-4}$, $\delta \approx 10$ and $\tau'_{\rm d} \approx \tau_{\rm d}$. The period of the low amplitude mass transfer cycles is therefore given by

$$\tau = \frac{2\pi}{\omega} \approx 0.02\,\sqrt{\tau_{\rm ce}\tau_{\rm d}}. \tag{92}$$

For higher braking rates, e.g., according to Verbunt & Zwaan (1981), mass transfer is stable. Only CVs with more massive donor stars can undergo mass transfer cycles for such a high braking rate. Fig. 13 shows the evolution

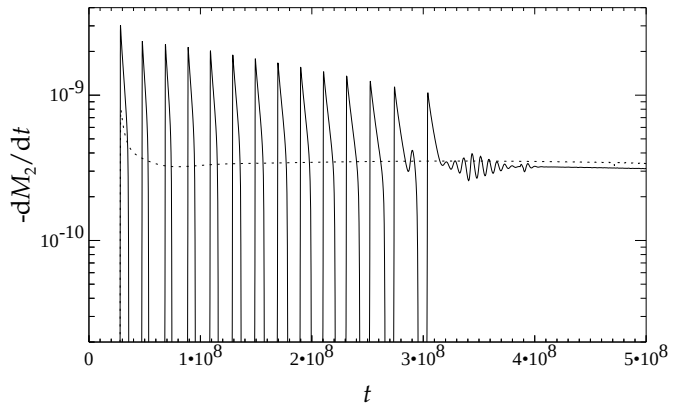

Figure 12. Mass transfer rate $-\dot{M}_2$ $[M_\odot/\mathrm{yr}]$ as function of time t [yr] for the same system as in Fig. 10. The computation stops at $M_2 \approx 0.34\,M_\odot$.

of a CV with an initially 1 $M_\odot$ MS donor. The stationary mass transfer rate becomes stable when the mass of the convective envelope $M_{\rm ce}$ and therefore $\tau_{\rm ce}$ becomes large enough (see also Ritter et al. 2000).

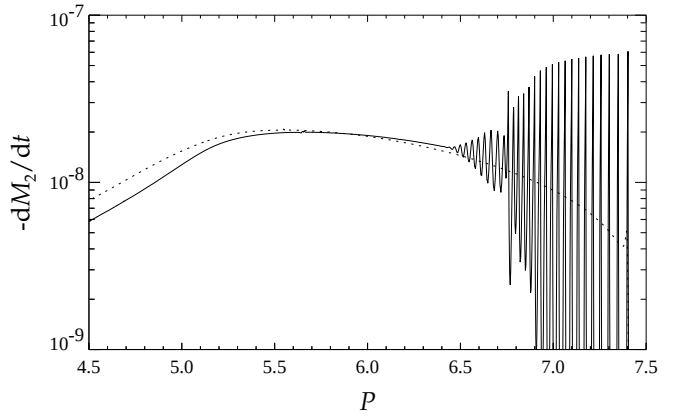

Figure 13. Mass transfer rate $-\dot{M}_2$ $[M_\odot/\mathrm{yr}]$ from a slightly evolved 1 $M_\odot$ MS star ($X_{\rm c} \approx 0.62$) onto a 0.8 $M_\odot$ white dwarf for the point source model as function of orbital period P [hr]. System parameters: $\overline{\eta} = 0$, $\nu = q$, $\alpha = 0.3$, and strong braking according to Verbunt & Zwaan (1981). The dotted line shows the evolution without irradiation feedback.

The dependence of the temporal evolution of mass transfer cycles on the efficiency parameter α is shown in fig. 14. The duration of the high state decreases with decreasing α until the mass transfer rate becomes sinusoidal with a frequency ω as given in (91). For even weaker feedback the oscillations are damped or even vanish completely.

6.1.2. Highly evolved MS donors

The timescale of central hydrogen burning for low-mass MS stars is much longer than a Hubble time. One way of ac-

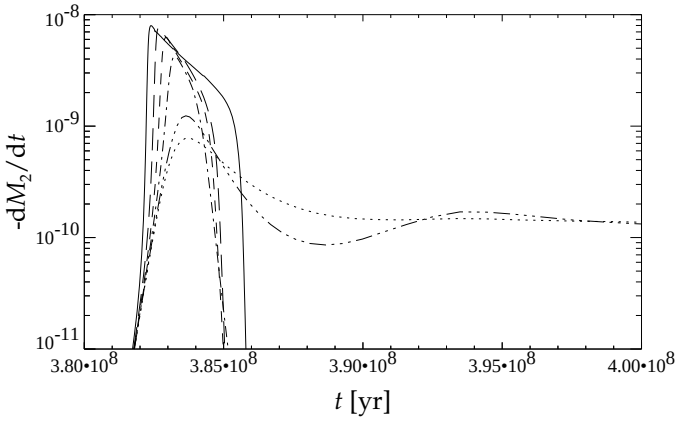

Figure 14. Mass transfer rate $-\dot{M}_2$ $[M_\odot/\mathrm{yr}]$ from an unevolved 0.5 $M_\odot$ MS star onto an 0.8 $M_\odot$ white dwarf for conservative mass transfer ($\overline{\eta} = 1$), $\dot{J} = \dot{J}_{\rm grav}$, and the constant flux model for $\alpha = 0.02$, 0.04, 0.1, 0.2, 0.4, and 1.0 (dotted, dot-dash-dotted, dash-dotted, short-dashed, long-dashed, and solid line, respectively) as function of time t [yr] .

counting for evolved low-mass donors in CVs is prior thermal timescale mass transfer from an evolved, initially more massive star. In this case the mass losing star is more massive to such an extent that the system is initially thermally unstable ($\zeta_{\rm e} - \zeta_{\rm R} < 0$) and the mass transfer occurs on a thermal timescale (Kolb et al. 2000; Schenker et al. 2002).

Although the bipolytrope model is formally valid only for chemically homogeneous stars we tentatively apply it also to chemically evolved donor stars. As an example fig. 15 shows s' and f for an 0.45 $M_\odot$ remnant of thermal timescale mass transfer with a central hydrogen abundance of $X_{\rm c} = 0.05$. It is the core of an initially more massive MS star of 1.6 $M_\odot$. According to (66) $\tau_{\rm ce}$ is less than $\frac{1}{10}$ of $\tau_{\rm ce}$ of an unevolved MS star of the same mass, and its radius is larger by $\sim 70\%$. Due to its deeper superadiabatic convection zone the maximum of s' is shifted to higher values of $\langle f_{\rm irr} \rangle$ and due to its larger radius f is also shifted to larger values of $\langle f_{\rm irr} \rangle$, but in total the difference to the case with an unevolved donor discussed before is comparatively small. As can be seen from fig. 15, this particular system should be stable for $\alpha = 0.1$ but can undergo cycles for $\alpha = 0.3$. When going to smaller donor masses or lower braking rates during the initial evolution also remnants of thermal timescale mass transfer can become unstable for $\alpha \gtrsim 0.1$ as CVs with unevolved donors do. It seems that CVs with an evolved donor are not more susceptible to mass transfer cycles than CVs with unevolved donors (if at all, it is the other way around). Rather they are susceptible at a shorter driving timescale $\tau_{\rm d}$.

As for unevolved CVs it is also possible to determine the range of $\tau_{\rm d}$ where mass transfer cycles should occur, e.g., if $\alpha = 0.3$:

$$3.5 \cdot 10^7\,\mathrm{yr} \lesssim \tau_{\rm d} \lesssim 3.5 \cdot 10^9\,\mathrm{yr}. \qquad (93)$$

According to this result such a system should undergo mass transfer cycles even for rather high braking rates. However,

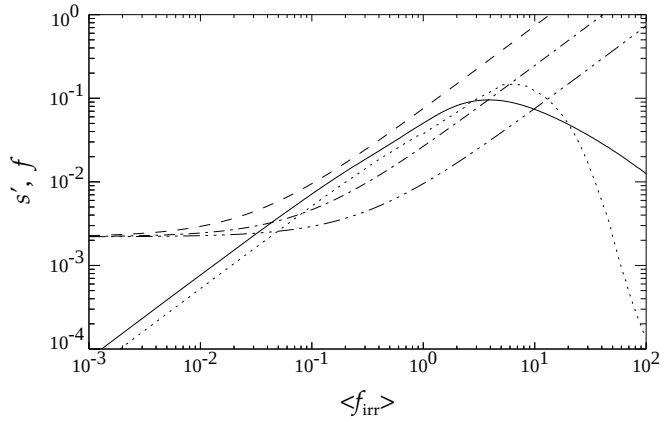

Figure 15. s' for a CV with an highly evolved $0.45\,M_\odot$ remnant of thermal timescale mass transfer (no. 4 of table 1) and an $0.86\,M_\odot$ white dwarf for the point source and constant flux model (solid and dotted line). s' is compared to f for $\overline{\eta} = 0.25$ and $\alpha = 0.1$, 0.3, and 1.0 (short-dashed, dash-dotted, and dot-dash-dotted line, respectively).

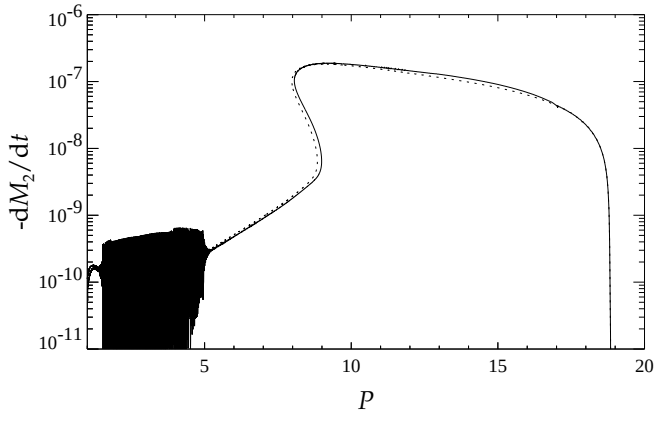

Figure 16. Mass transfer rate $-\dot{M}_2$ $[M_\odot/\mathrm{yr}]$ from an evolved initially $1.6\,M_\odot$ MS star (no. 4 of table 1) onto an initially $0.6\,M_\odot$ white dwarf for the point source model as function of orbital period P [hr]. System parameters: $\overline{\eta} = 0.25$, $\nu = q$, $\alpha = 0.3$, and strong braking according to Verbunt & Zwaan (1981). The dotted line shows the evolution without irradiation feedback. The onset of mass transfer cycles occurs at $M_1 \approx 0.91\,M_\odot$ and $M_2 \approx 0.26\,M_\odot$.

fig. 16 shows[6] that this is not the case, when the donor star reaches $M_2 = 0.45\,M_\odot$ at an orbital period of $\sim 8\,\mathrm{hr}$. Instead, the system becomes unstable at a donor mass much lower than expected, i.e., at about $0.26\,M_\odot$. The reason for this discrepancy is probably that the bipolytrope model underestimates the timescale $\tau_{\rm ce}$ on which the stellar radius changes if irradiation is changed. Numerical computations indicate that $\tau_{\rm ce}$ from (66) is too large by a factor of ~ 1.4 for a fully convective $0.3\,M_\odot$ MS star whereas it is too small by ~ 1.6 for an $0.5\,M_\odot$ MS star and even more so for more massive or more evolved stars. As a result evolved systems are significantly more stable than previously expected.

6.1.3. Giant donors

Another group of CVs are systems containing a giant or subgiant donor. Fig. 17 shows the stability diagram for a CV with a giant donor of $0.8\,M_\odot$ (model no. 6 of table 1). Since $\tau_{\rm ce}$ according to (66) gives an unreliable estimate for the thermal timescale of the convective envelope of giants, we have used the timescale $\tau_{\rm ce,U} \sim 6 \cdot 10^3\,\mathrm{yr}$ which is defined as the thermal energy U of the convective envelope divided by the stellar luminosity. The timescale on which the giant radius changes, when irradiation is changed, is even larger than $\tau_{\rm ce,U}$ by ~ 2. Giants typically have $\frac{H_{\rm p}}{R_2} \sim 10^{-2}$ and $\delta \sim n + 5 \approx 2$. In our case for $\alpha = 0.3$ the "island of instability" ranges from 0.25 to 20 in $\langle f_{\rm irr}\rangle$. This means the ratio of $\tau_{\rm ce}$ and $\tau'_{\rm d}$ must be in the range

$$8.5 \cdot 10^{-4} \lesssim \frac{\tau_{\rm ce}}{\tau'_{\rm d}} \lesssim 7 \cdot 10^{-2}, \tag{94}$$

or taking into account (89)

$$5.5 \cdot 10^{-4} \lesssim \frac{\tau_{\rm ce}}{\tau_{\rm d}} \lesssim 4 \cdot 10^{-2}. \tag{95}$$

Using analytical approximations given by Ritter (1999, eq. 43) and (42) we can write

$$\frac{\tau_{\rm ce}}{\tau_{\rm d}} \approx -3 \cdot 10^{-4} \frac{M_2 - M_{\rm c}}{M_2} \left(\frac{M_2}{M_\odot}\right)^2 \left(\frac{0.25\,M_\odot}{M_{\rm c}}\right)^6 \tag{96}$$

for Pop. I giants and a similar expression for Pop. II giants. The temporal evolution of the core mass $M_{\rm c}$ is given by

$$M_{\rm c} = M_{\rm c,i}\left(1 - \frac{t}{t_\infty}\right)^{-\frac{1}{7}}. \tag{97}$$

Here, $M_{\rm c,i}$ denotes the initial core mass and t_∞ the nuclear timescale, i.e., the time when the core mass formally becomes infinite. Almost all values on the right-hand side of (96) are less than unity. We have $M_{\rm c} < M_2$ and for thermally stable systems typically $M_2 < M_\odot$. Accordingly, $\frac{\tau_{\rm ce}}{\tau_{\rm d}}$ is too small for destabilizing the system except if $M_{\rm c} < 0.25\,M_\odot$ and $M_{\rm c} \ll M_2$.

For the system shown in fig. 17 Eq. (96) yields:

$$\frac{\tau_{\rm ce}}{\tau_{\rm d}} \approx 5 \cdot 10^{-5}. \tag{98}$$

In fact, to destabilize the system α would have to be larger by about an order of magnitude than the value of 0.3 which we have chosen for this example. Since an efficiency $\alpha > 1$ is rather unrealistic, we conclude that CVs with extended giants can not undergo mass transfer cycles.

[6] To perform the evolutionary computations shown in figs. 16 and 22 from the initial turn-on of mass transfer to the minimum period without any discontinuity we used opacity tables for solar composition in the outer layers. Comparisons with computations using correct Helium and CNO abundances for the final mass transfer phase indicate that, though using "incorrect" opacity tables in that evolutionary stage leads to a different stellar radius, it does not affect the mass transfer cycles significantly.

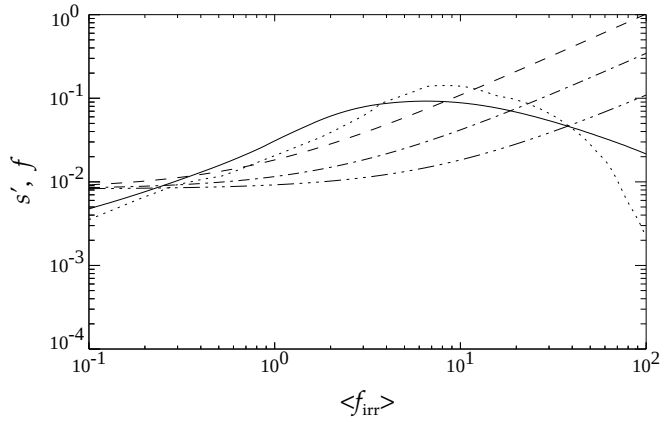

Figure 17. s' for a CV with an $0.8\,M_\odot$ giant (no. 6 of table 1) and an $1.2\,M_\odot$ white dwarf for the point source and the constant flux model (solid and dotted line). s' is compared to f for $\overline{\eta} = 0$ and $\alpha = 0.1$, 0.3, and 1.0 (short-dashed, dash-dotted, and dot-dash-dotted line, respectively).

There are three reasons, why CVs with giant donors are the more stable, the more extended the giants are: First, King et al. (1997) have neglected the last term in (79) that restricts the region of instability not only to high but also to low braking rates. Thus, systems do not get automatically unstable for sufficiently small braking rates. Second, the depth of the superadiabatic convection zone grows during giant evolution which shifts the "island of instability" to higher $\langle f_{\rm irr}\rangle$. Hence, more evolved giants are less affected by irradiation. Third, more evolved giants have a larger scale height $\frac{H_{\rm p}}{R_2}$ so that their "island of instability" is smaller than for less evolved giants.

6.2. Low-mass X-ray binaries

6.2.1. Unevolved MS donors

As we have discussed in the last section, CVs might undergo mass transfer cycles for $0.1 \lesssim \alpha \lesssim 1$ given a suitable driving timscale. Another class of compact binary systems with thermally stable mass transfer, i.e., small q, are LMXBs. In the following we consider only LMXBs with neutron star primaries. In principle, the discussion for these system is analogous to the discussion of CVs. While the radius of a white dwarf is about $10^{-2}\,R_\odot$, the radius of a neutron star is only about 10 km. Since for a given secondary star and driving mechanism $\langle f_{\rm irr}\rangle \sim \frac{\alpha}{R_1}$ (cf. Eq. (84)) the smaller radius of a neutron star has to be compensated by a correspondingly small value of α for achieving a comparable value of $\langle f_{\rm irr}\rangle$. Because an efficiency that small is unlikely, King et al. (1996, 1997); Ritter et al. (2000) have concluded that irradiation in LMXBs is too strong to destabilize such systems.

However, this conclusion applies only to the constant flux model but not to the point source model. For the point source model s' decreases much more slowly for large $\langle f_{\rm irr}\rangle$ than for the constant flux model because the surface elements near the terminator are only partially blocked by irradiation, even for very high fluxes due to the high angle of incidence. Therefore, the point source model does not require $\langle f_{\rm irr}\rangle \sim 1$ to get mass transfer cycles. Instead, s' becomes larger than f for fluxes below $\langle f_{\rm irr}\rangle \lesssim 10^2 - 10^3$ as can be seen in fig. 18 for a LMXBs with an unevolved donor, in fig. 19 for a LMXBs with a remnants of thermal timescale mass transfer, and in fig. 20 for a LMXBs with a giant. Thus, LMXBs can become unstable for $\alpha \lesssim 10^{-2} - 10^{-1}$.

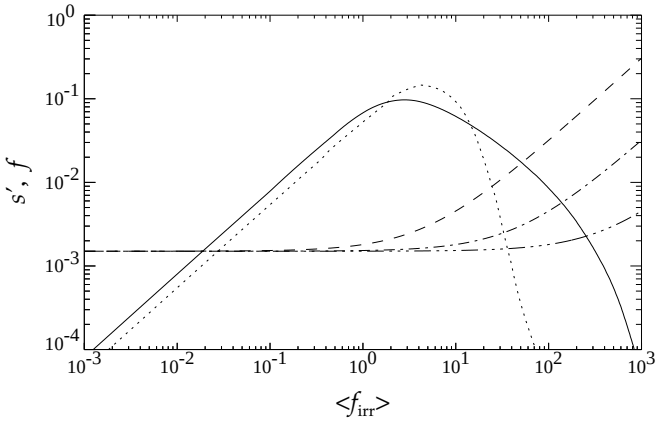

Figure 18. s' for an LMXB with an unevolved $0.8\,M_\odot$ MS star (no. 3 of table 1) and an initially $1.4\,M_\odot$ NS for the point source and the constant flux model (solid and dotted line). s' is compared to f for $\overline{\eta} = 1$ and $\alpha = 0.01$, 0.1, and 1.0 (short-dashed, dash-dotted, and dot-dash-dotted line, respectively).

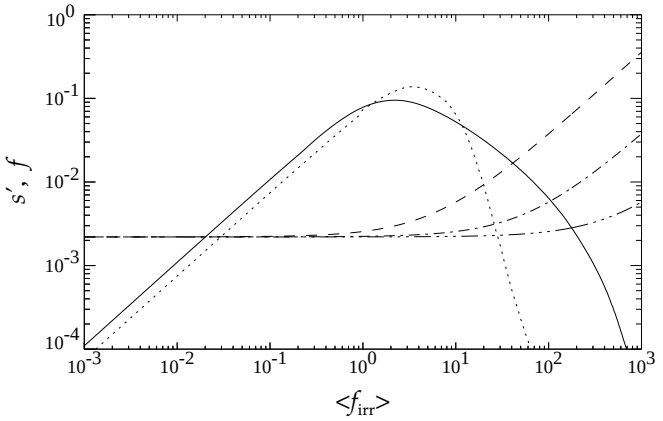

Figure 19. s' for an LMXB with an $0.6\,M_\odot$ remnant of thermal timescale mass transfer (no. 5 of table 1) and an initially $1.4\,M_\odot$ NS for the point source and the constant flux model (solid and dotted line). s' is compared to f for $\overline{\eta} = 1$ and $\alpha = 0.01$, 0.1, and 1.0 (short-dashed, dash-dotted, and dot-dash-dotted line, respectively).

The "island of instability" for the LMXB with an unevolved donor, which is shown in fig. 18, ranges from 0.02 to 150 in $\langle f_{\rm irr}\rangle$ for $\alpha = 0.1$. This corresponds to

$$6 \cdot 10^{-7} \lesssim \frac{\tau_{\rm ce}}{\tau'_{\rm d}} \lesssim 4.5 \cdot 10^{-3}. \qquad (99)$$

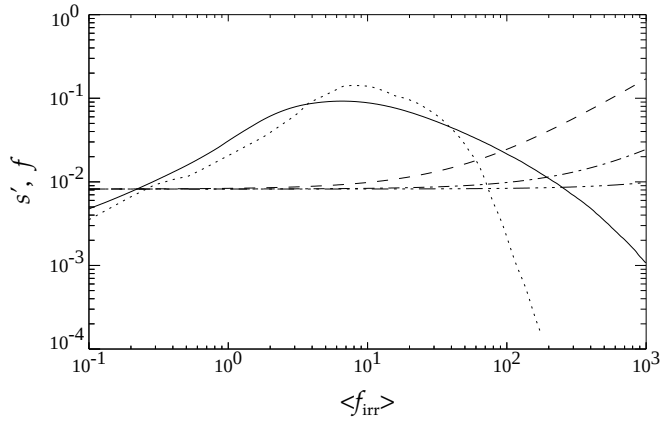

Figure 20. s' for an LMXB with an $0.8\,M_\odot$ giant (no. 6 of table 1) and an initially $1.4\,M_\odot$ NS for the point source and the constant flux model (solid and dotted line). s' is compared to f for $\overline{\eta} = 1$ and $\alpha = 0.01$, 0.1, and 1.0 (short-dashed, dash-dotted, and dot-dash-dotted line, respectively).

With $\tau_{\rm ce} \approx 2 \cdot 10^6\,$yr for an unevolved $0.8\,M_\odot$ MS star and using (89) we get

$$4.5 \cdot 10^8\,\mathrm{yr} \lesssim \tau_{\rm d} \lesssim 3.5 \cdot 10^{12}\,\mathrm{yr}. \qquad (100)$$

From this we can infer that for $\alpha = 0.1$ such a system shows cycles for gravitational braking with $\tau_{\rm grav} = \frac{\tau_{\rm J}}{2} \approx 6 \cdot 10^9\,$yr and also for higher braking rates of up to $10\dot{J}_{\rm grav}$. Numerical computations show that this system is rather near to the boundary of the unstable zone. Since the bipolytrope model underestimates $\tau_{\rm ce}$ by a factor of ~ 2, the system undergoes cycles only for braking rates up to $5\dot{J}_{\rm grav}$. Only low-amplitude sinusoidal oscillations occur for $\alpha = 0.1$ while for $\alpha = 10^{-2}$ the system is deep in the unstable region as the evolution in fig. 21 demonstrates.

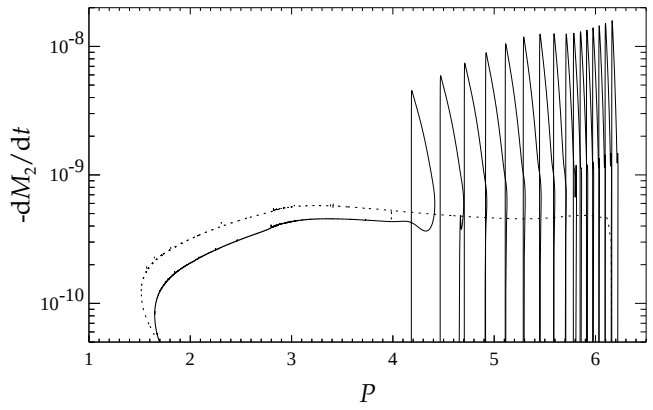

Figure 21. Mass transfer rate $-\dot{M}_2$ $[M_\odot/\mathrm{yr}]$ from an evolved ($X_{\rm c} \approx 0.66$) initially $0.8\,M_\odot$ MS star onto an initially $1.4\,M_\odot$ neutron star for the point source model as function of orbital period P [hr]. System parameters: $\overline{\eta} = 1$, $\alpha = 0.01$, and strong braking according to Verbunt & Zwaan (1981). The dotted line shows the evolution without irradiation feedback.

6.2.2. Highly evolved MS donors

There is only a small region in the parameter space where LMXBs can undergo significant cycles for an irradiation efficiency as large as ~ 0.1 and for high braking rates according to Verbunt & Zwaan (1981). As an example we show in fig. 19 the evolution of a LMXB through thermal timescale mass transfer. The "island of instability" for the $0.6\,M_\odot$ remnant (model no. 5 of table 1), corresponding to an orbital period of $\sim 8\,$hr, is shown in fig. 22 and ranges from 0.02 to 100 in $\langle f_{\rm irr}\rangle$, corresponding to

$$7 \cdot 10^{-7} \lesssim \frac{\tau_{\rm ce}}{\tau'_{\rm d}} \lesssim 3.5 \cdot 10^{-3}. \qquad (101)$$

With $\tau_{\rm ce} \approx 5 \cdot 10^5\,$yr the driving timescale $\tau_{\rm d}$ must be between $2 \cdot 10^8\,$yr and $10^{12}\,$yr so that the system should be near the boundary of the unstable region. This is roughly consistent with the fact that the system becomes stable just one cycle later at $P \sim 7\,$hr.

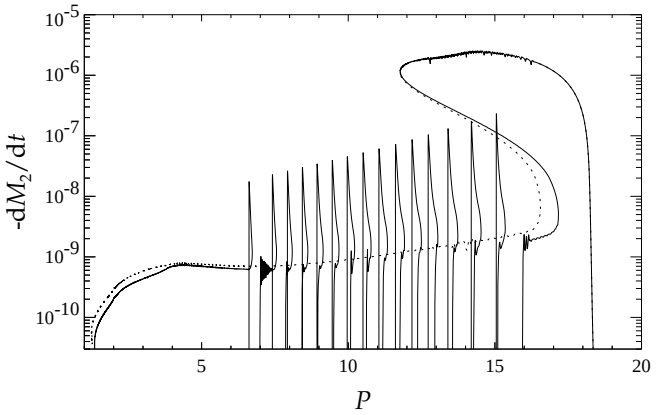

Figure 22. Mass transfer rate $-\dot{M}_2$ $[M_\odot/\mathrm{yr}]$ from an evolved, initially $3.0\,M_\odot$ MS star (no. 5 of table 1) onto an initially $1.4\,M_\odot$ neutron star for the point source model and $\alpha = 0.1$ as function of orbital period P [hr]. For this computation $\overline{\eta} = \eta = 1$ has been used as long as the Eddington accretion rate of the neutron star $\left(2 \cdot 10^{-8}\,\dot{M}_\odot/\mathrm{yr}\right)$ is not exceeded, otherwise $\overline{\eta} = \eta < 1$. The dotted line shows the evolution of the same system without irradiation feedback.

6.2.3. Giant donors

Unlike CVs with giant donors LMXBs with giant donors can undergo mass transfer cycles even for very extended giants. This can be seen from the example shown in fig. 20 which illustrates the conditions at the beginning of the evolution shown in Figs. 23 and 24. Unlike all other evolutions shown before this system evolves to longer orbital periods because it is driven by nuclear evolution, not loss of angular momentum.

However, taking into account, that a neutron star has a quite small Eddington accretion rate of $\sim 2 \cdot 10^{-8}\,M_\odot/\mathrm{yr}$, this particular giant system would be stable, since the secular mass

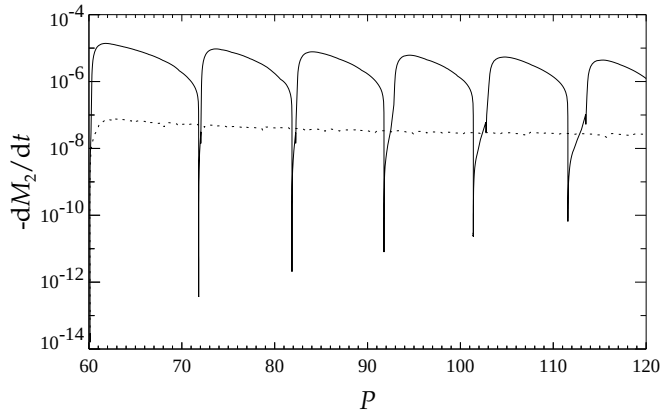

Figure 23. Mass transfer rate $-\dot{M}_2$ [$M_\odot$/yr] from an $0.8\,M_\odot$ giant (no. 6 of table 1) onto an initially $1.4\,M_\odot$ neutron star for the point source model, $\overline{\eta} = 1$, and $\alpha = 0.1$ as function of orbital period P [d]. The dotted line shows the evolution of the same system without irradiation feedback.

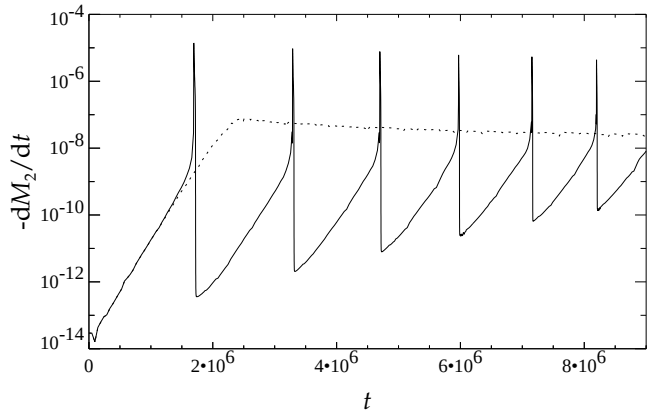

Figure 24. Same as fig. 23 but $-\dot{M}_2$ as function of time t [yr].

transfer rate is above the Eddington rate, so that there would be no irradiation feedback.

6.3. General outline of mass transfer cycles and observational implications

The appearance of mass transfer cycles differs between different types of systems. "Ideal" outbursts as outlined by King et al. (1997) require a very short ratio of $\tau_{\rm ce}$ and $\tau'_{\rm d}$ which is typical for giants. They are characterised by a very short high state at a rather high mass transfer rate followed by a long lasting low state as shown by fig. 24.

In the limit of weak irradiation feedback, as it is typically the case for CVs with $0.1 \lesssim \alpha \lesssim 1$ and weak braking, a system leaves the high state long before saturation is reached. Only a few 10^{-3} of the stellar mass is transferred during a cycle and the recurrence timescale is rather short. In the limit of strong irradiation feedback, as it is often the case for LMXBs with $10^{-2} \lesssim \alpha \lesssim 0.1$, the system stays in the high state until saturation has been almost exactly reached. As a consequence of this, the mass transfer rate decreases to almost the stationary value before the system enters the low state. The duration of the high and low state are of the same order, and in the high state the system transfers mass just slightly above the stationary mass transfer rate for most of the time.

Since the timescale of mass transfer cycles, i.e., the thermal timescale of the convective envelope of the donor is by far longer than typical observational timescales (at most of order of centuries), it is effectively not possible to observe the evolution of a single system from the high into the low state, or vice versa. Nevertheless, the occurrence of these cycles would affect the observable properties of a binary population. First, systems in the low state are more difficult to observe than in the bright high state or may even appear as detached systems if mass transfer ceases completely in the low state. If the duration of the low state is longer than that of the high state, then most of the population can be basically unobservable. Second, even in the high state the mass transfer does not proceed at a constant rate but declines continuously from the peak rate until the system "switches" into the low state. Hence, even a completely homogeneous sample can show significant variations in the mass transfer rate. Third, the mean mass transfer rate of the observable systems in the high state can be significantly larger than the secular mass transfer rate which can lead to apparent discrepancies between observations and theoretical predictions if the occurrence of mass transfer cycles is not taken into account.

Therefore, mass transfer cycles could provide an explanation for, e.g., the scatter of mass transfer rates of novalike CVs above the period gap, the disappearance of bright systems at the upper edge of the period gap, or discrepancies between predicted and observed luminosities and birthrates of LMXBs as recently suggested by Pfahl et al. (2003).

6.4. Non-local effects

We have assumed that irradiation is a local effect and can be treated for every surface element of the donor separately. If the contribution of non-local effects (e.g., circulations) to the lateral heat transport becomes non-negligible for sufficiently strong irradiation, or if there is another mechanism which heats the unilluminated side (e.g., scattering of X-rays by an extended X-ray corona), then also the effective temperature and the intrinsic flux on the unilluminated surface depends on $\langle f_{\rm irr} \rangle$ and differs from T_0 and F_0, respectively.

Observations of the eclipsing binary AA Dor show that even in the case of very strong irradiation an illuminated star can preserve a cool hemisphere with $\sim 2\,000$ K while the illuminated side is heated up to $\sim 20\,000$ K (Hilditch et al. 2003). Therefore, it seems plausible that also in the case of LMXBs at most a small fraction of the irradiating flux is transported to the unilluminated side. Nevertheless, for sufficiently strong irradiation, e.g., $\langle f_{\rm irr} \rangle \sim 10^4$, even a small fraction can have a significant effect onto the unilluminated side. We note that with the general definition of s in (18) our analytical ansatz remains valid, even if the unilluminated side is heated up, and we formally get the same stability criterion. In this case the

shape of s' depends on the exact prescription of those non-local effects. Here we can not make any quantitative predictions. Nevertheless, it is plausible that s' becomes greater at higher fluxes $\langle f_{\rm irr} \rangle$ if non-local effects are taken into account. This would mean that our local treatment of irradiation provides a lower limit on the occurrence of mass transfer cycles in LMXBs. An upper limit is given by the fact that the area below the s' curve has to be less than the maximum fraction of the surface which is affected by irradiation, i.e., less than unity.

7. Summary and Conclusion

We have described the physics of irradiation driven mass transfer cycles by a two-dimensional system of ordinary differential equations similar to King et al. (1996). An additional term of order of several times $\frac{H_{\rm p}}{R_2}$ which reflects the usual thermal relaxation of the mass losing star, can not be neglected, because it provides an upper limit for the driving timescale $\tau_{\rm d}$, respectively a lower limit for the timescale ratio $\frac{\tau_{\rm ce}}{\tau'_{\rm d}}$, where mass transfer cycles can occur. Taking into account this term and also the rather large pressure scale height and the deep superadiabatic convection zone of giants we have concluded that CVs with giants above a certain core mass can not undergo mass transfer cycles unless the efficiency parameter α is unexpectedly large. On the other hand LMXBs with giants might be susceptible to the irradiation instability as it has been predicted by King et al. (1997).

We agree with results of King et al. (1996); Ritter et al. (2000) regarding CVs with unevolved MS stars: For high braking rates (e.g., Verbunt & Zwaan 1981), as they are also required by the period gap model (e.g., Spruit & Ritter 1983; Kolb 1993), such systems are stable except for the most massive ($\sim 1\,M_\odot$) donor stars. On the other hand, for low braking rates, as they are proposed by Sills et al. (2000); Andronov et al. (2003), CVs above the period gap might undergo cycles. In this case only novalikes are affected since dwarf novae have rather large amplitude outbursts with a rather small duty cycle and therefore a small $\alpha_{\rm d}$. Even for gravitational braking the susceptability to irradiation ceases within the period gap so that CVs with unevolved MS stars below the period gap are stable.

Numerical evolutionary computations have shown that the uncritical application of the predictions of the analytical model to highly evolved remnants of thermal timescale mass transfer does not yield good quantitative estimates for the boundaries of the unstable region. The timescale on which the stellar radius changes, if irradiation is changed, seems to be significantly underestimated by the bipolytrope model so that such systems are more stable at high braking rates than previously expected. The most evolved systems are susceptible to irradiation for $0.1 \lesssim \alpha \lesssim 1$ and orbital periods roughly between 2 and 5 hours, or donor masses between 0.1 and $0.3\,M_\odot$, respectively. For giants the ratio of thermal energy of the envelope divided by the stellar luminosity seems to give a good estimate for $\tau_{\rm ce}$.

Since in the point source model surface elements near the terminator are irradiated at a high angle of incidence, they are only partially blocked by irradiation even for high fluxes. Thus, other than expected by King et al. (1996, 1997); Ritter et al. (2000) also LMXBs with unevolved or evolved MS stars might be susceptible to the irradiation instability. Regarding the driving timescale for such systems basically the same restrictions apply as for CVs. LMXBs can undergo mass transfer cycles only for $\alpha \lesssim 0.1$. The contribution of non-local effects of irradiation, e.g., circulations, which were not taken into account by our model, might be non-negligible for LMXBs. It seems plausible that this effect tendentially destabilizes the mass transfer. However, it is not clear in all cases whether mass transfer in LMXBs is driven by Roche lobe overflow or by irradiation-induced winds (Basko & Sunyaev 1973; Basko et al. 1977; Iben Jr. et al. 1997). In the latter case our model could obviously not be applied to these systems.

We conclude that the analytical model gives a qualitatively and also quantitatively suitable description for the onset of mass transfer cycles except for highly evolved remnants of thermal timescale mass transfer. We think that the boundaries of the unstable regions can be determined with an accuracy of a factor of $\lesssim 2$.

To answer the final question whether the observable CV or LMXB population or parts of it is undergoing mass transfer cycles we need to know two basic parameters: the driving timescale, respectively the magnetic braking law, and the efficiency α. Nevertheless, we have shown that irradiation-driven mass transfer cycles in compact binaries are possible for not unreasonable values of α and $\tau_{\rm d}$.

Acknowledgements. We thank A. Weiss and H. Schlattl for providing us with their stellar evolutionary code, H. Schlattl for valuable support and helpful discussions about numerics, I. Baraffe for providing high resolution EOS tables, P. P. Eggleton for providing us with his EOS code, P. H. Hauschildt and J. W. Ferguson for providing opacity tables, and J.-M. Hameury for providing high resolution irradiation tables. We also thank our referee P. Podsiadlowski for his helpful comments and suggestions.

References

Adelberger, E. G., Austin, S. M., Bahcall, J. N., et al. 1998, Rev. Mod. Phys., 70, 1265
Alexander, D. R. & Ferguson, J. W. 1994, ApJ, 437, 879
Andronov, N., Pinsonneault, M., & Sills, A. 2003, ApJ, 582, 358
Barman, T. S. 2002, Ph.D., University of Georgia
Barman, T. S. & Hauschildt, P. H. 2001, in ASP Conf. Ser., Vol. 231, Galactic Structure, Stars and the Interstellar Medium, ed. C. E. Woodward, M. D. Bicay, & J. M. Shull (San Francisco: Astron. Soc. Pac.), 447–449
Barman, T. S. & Hauschildt, P. H. 2002, in ASP Conf. Ser., Vol. 261, The Physics of Cataclysmic Variables and Related Objects, ed. B. T. Gänsicke, K. Breuermann, & K. Reinsch (San Francisco: Astron. Soc. Pac.), 49–52
Basko, M. M., Hatchett, S., McCray, R., & Sunyaev, R. A. 1977, ApJ, 215, 276
Basko, M. M. & Sunyaev, R. A. 1973, Ap&SS, 23, 117
Benvenuto, O. G. & de Vito, M. A. 2003, MNRAS, 342, 50
Böhm-Vitense, E. 1958, Z. f. Astrophys., 46, 108
Brett, J. M. & Smith, R. C. 1993, MNRAS, 264, 641

Büning, A. 2003, Ph.D., Ludwig-Maximilians-Universität München
Caughlan, G. R., Fowler, W. A., Harris, M. J., & Zimmerman, B. A. 1985, Atomic Data and Nuclear Data Tables, 32, 197ff
Cox, J. P. & Giuli, R. T. 1968, Principles of Stellar Structure I/II (New York, London, Paris: Gordon and Breach, Science Publishers)
Eddington, A. S. 1926, MNRAS, 86, 320
Guckenheimer, J. & Holmes, P. 1983, in Applied Mathematical Sciences, Vol. 42, Nonlinear Oscillations, Dynamical Systems, and Bifurcations of Vector Fields (New York: Springer-Verlag)
Hameury, J.-M. 1996, A&A, 305, 468
Hameury, J.-M., King, A. R., Lasota, J. P., & Livio, M. 1989, MNRAS, 237, 835
Hameury, J.-M., King, A. R., Lasota, J.-P., & Raison, F. 1993, A&A, 277, 81
Hameury, J.-M. & Ritter, H. 1997, A&A, 123, 273
Hilditch, R. W., Kilkenny, D., Lynas-Gray, A. E., & Hill, G. 2003, MNRAS, 344, 644
Iben Jr., I., Tutukov, A. V., & Fedorova, A. V. 1997, ApJ, 486, 955
Iglesias, C. A. & Rogers, F. J. 1996, ApJ, 464, 943
King, A. R., Frank, J., Kolb, U., & Ritter, H. 1995, ApJ, 444, L37
King, A. R., Frank, J., Kolb, U., & Ritter, H. 1996, ApJ, 467, 761
King, A. R., Frank, J., Kolb, U., & Ritter, R. 1997, ApJ, 482, 919
King, A. R. & Kolb, U. 1995, ApJ, 439, 330
Kippenhahn, R. & Weigert, A. 1990, Stellar Structure and Evolution (Berlin: Springer-Verlag)
Kippenhahn, R., Weigert, A., & Hofmeister, E. 1967, in Methods in Computational Physics, Vol. 7, Astrophysics, ed. B. Alder, S. Fernbach, & M. Rosenberg (New York: Academic Press), 129–190
Kolb, U. 1993, A&A, 271, 149
Kolb, U., Davies, M. B., King, A., & Ritter, H. 2000, MNRAS, 317, 438
Kolb, U. & Ritter, H. 1992, A&A, 254, 213
McCormick, P. & Frank, J. 1998, ApJ, 500, 923
Mochnacki, S. W. 1984, ApJS, 55, 551
Nordlund, Å. & Vaz, L. P. R. 1990, A&A, 228, 231
Paczyński, B. 1971, ARA&A, 9, 183
Pfahl, E., Rappaport, S., & Podsiadlowski, P. 2003, ApJ, 597, 1036
Podsiadlowski, P. 1991, Nature, 350, 136
Pols, O. R., Tout, C. A., Eggleton, P. P., & Han, Z. 1995, MNRAS, 274, 964
Prialnik, D. & Kovetz, A. 1995, ApJ, 445, 789
Renvoizé, V., Baraffe, I., Kolb, U., & Ritter, H. 2002, A&A, 389, 485
Ritter, H. 1988, A&A, 202, 93
Ritter, H. 1994, Mem. Soc. Astron. Ital., 65, 173
Ritter, H. 1999, MNRAS, 309, 360
Ritter, H. & Kolb, U. 2003, A&A, 404, 301
Ritter, H., Zhang, Z., & Hameury, J.-M. 1996, in Cataclysmic Variables ans Related Objects, ed. A. Evans & J. H. Wood, Proceedings of the 158th Colloquium of the IAU (Dordrecht: Kluwer Academic Publishers)
Ritter, H., Zhang, Z., & Kolb, U. 1995, in Cataclysmic Variables, ed. A. Bianchini, M. della Valle, & M. Orio (Dordrecht: Kluwer Academic Publishers), 479–486
Ritter, H., Zhang, Z.-Y., & Kolb, U. 2000, A&A, 360, 959
Ruciński, S. M. 1969, Acta Astron., 19, 245
Saumon, D., Chabrier, G., & van Horn, H. M. 1995, ApJS, 99, 713
Schenker, K., King, A. R., Kolb, U., Wynn, G. A., & Zhang, Z. 2002, MNRAS, 337, 1105
Schenker, K., Kolb, U., & Ritter, H. 1998, MNRAS, 297, 633
Schlattl, H. 1999, Ph.D., Technische Universität München
Schlattl, H., Weiss, A., & Ludwig, H.-G. 1997, A&A, 322, 646
Sills, A., Pinsonneault, M. H., & Terndrup, D. M. 2000, ApJ, 534, 335
Spruit, H. C. 1982, A&A, 108, 348
Spruit, H. C. & Ritter, H. 1983, A&A, 124, 267
Tout, C. A., Eggleton, P. P., Fabian, A. C., & Pringle, J. E. 1989, MNRAS, 238, 427
Vaz, L. P. R. 1985, Ap&SS, 113, 349
Vaz, L. P. R. & Nordlund, Å. 1985, A&A, 147, 281
Verbunt, F. & Zwaan, C. 1981, A&A, 100, L7
Wagenhuber, J. & Weiss, A. 1994, A&A, 286, 121
Webbink, R. F. 1985, in Cambridge Astrophysics Series, Vol. 6, Interacting Binary Stars, ed. J. E. Pringle & R. A. Wade (Cambridge: Cambridge University Press), 39–70
Zahn, J.-P. 1977, A&A, 57, 383